



DEGREE PROJECT IN SYSTEM MATHEMATICS,
SECOND CYCLE, 30 CREDITS
STOCKHOLM, SWEDEN 2022

Development of Acoustic Simulation Methods for Exhaust Systems

KTH Thesis Report

Christin Friberg Femling

Degree Project in Systems Engineering (30 ECTS credits)
Master's Programme in Applied and Computational Mathematics
KTH Royal Institute of Technology, School of Engineering Sciences
Stockholm, Sweden, 2021

Author

Christin Friberg Femling

External Partner

Scania CV AB

Examiner

Per Enqvist, KTH Royal Institute of Technology

Supervisors

Per Enqvist, KTH Royal Institute of Technology
Naveen Indolia, Scania CV AB

Abstract

Noise pollution is a growing concern due to its harmfulness to human health. Heavy vehicles powered by internal combustion engines stands for a major part of the environmental noise, why noise reduction is an increasing priority in engine development. Within this study, an optimization problem is posed in order to minimize acoustic output without impairing the engine's overall performance.

In our quest to diversify our noise reduction strategies, innovative ways of investigating this complex subject are essential. Here, we use simulations to investigate the possibility to reduce noise by component settings, as well as methods available to achieve that.

Regarding the methods, the results indicate that a built in optimization tool within the simulation software used works well, despite the high complexity of the problem. A significant noise reduction is achieved when adjusting the settings of two of the parameters studied.

This is a first attempt to tackle noise reduction in internal combustion engines by component settings. From the promising results, further improvements are expected as the simulation methods are refined and more components can be investigated accurately.

Keywords

Optimization, Acoustic Optimization, Systems Engineering, Engine Acoustics, Vehicle Acoustics, Internal Combustion Engine Acoustics, Exhaust Orifice Noise, Pass-by Noise

UTVECKLING AV AKUSTISKA SIMULERINGSMETODER FÖR AVGASSYSTEM

Sammanfattning

Bullerreducering är en allt viktigare fråga i samhället idag på grund av den negativa påverkan oljud kan ha på vår hälsa. Tunga fordon som drivs av förbränningsmotorer står för den största delen av buller i vår omgivning, varför bullerreducering är ett alltmer prioriterat område vid utveckling av dessa motorer och fordon. I denna studie arbetar vi utifrån ett optimeringsproblem för att minimera ljudnivåerna utan att försämra motorns övergripande prestanda.

I vår strävan att diversifiera strategier för bullerreducering behövs innovativa sätt att undersöka detta komplexa problem. Här används ett simuleringsverktyg för att undersöka möjligheterna att reducera ljudnivåerna genom att justera komponenternas beskaffenhet. Metoderna för att uppnå detta undersöks och utvärderas också.

Resultaten pekar på att ett inbyggt optimeringsverktyg i det simuleringsprogram som används hanterar optimeringsproblemet väl, trots dess höga komplexitet. En signifikant bullerreducering uppnås genom justering av inställningar hos två av de komponenter som undersökts.

Detta är ett första försök att hantera bullerreducering inom förbränningsmotorer genom simulering av olika komponentinställningar. Med tanke på de lovande resultaten från denna första undersökning förväntas ytterligare förbättringar om simuleringsmodellen kan förfinas och fler komponenter kan undersökas.

Nyckelord

Optimering, Akustisk Optimering, Systemteknik, Motorakustik, Fordonsakustik, Akustik hos Förbränningsmotorer, Avgasljud.

Acknowledgements

I would first like to thank my supervisor at KTH, Associate Professor Per Enqvist of the Department of Mathematics. Your insightful feedback has helped me raise the quality of the work to a higher level.

I would also like to extend my deepest gratitude to Brand Chief Engineer Naveen Indolia at Scania. Thank you for giving me the opportunity to work on this project, all the support and valuable advice throughout the work and that you so generously shared your extensive knowledge. I have learnt a lot from you and our discussions.

I am very grateful to the NXPS-team at Scania for the warm welcome to your group and for sharing your thoughts and ideas to improve my work. Special thanks to Pontus Gräsberg for always being available for my (many) questions and to Kim Petersson for your constructive and well-founded feedback. Outside the NXPS-team at Scania, I would like acknowledge Joakim Rodebäck, Johan Dahlqvist, and Fabrizio Sciuto for sharing your time and knowledge to help me execute this project and improve my work.

Finally, I must express my very profound gratitude to my beloved family and friends for always believing in me and supporting me throughout my years of study and through the process of writing this thesis. Pappa Bengt, thank you for explaining to me how an engine works in such a good way. I am impressed and humbled by your knowledge. And to my beloved husband Calle, thank you for your endless love and patience, for your constant encouragement and support and for being my rock.

Stockholm, January 2022

Christin Friberg Femling

Acronyms and abbreviations

GA	Genetic Algorithm
CMA-ES	Covariance Matrix Adaption Evolution Strategy
IC	internal combustion
DFT	discrete Fourier transform
CI	compression ignition
SI	spark ignition
RPM	revolutions per minute
RMS	root mean squared
GVW	gross vehicle weight
EGR	exhaust gas re-circulation
HGR	hot gas re-circulation
DoE	design of experiment
WHO	World Health Organisation
BSFC	brake-specific fuel consumption
SPL	sound pressure level
FFT	fast Fourier transform
TC	top center
BC	bottom center
PDE	partial differential equations
PID	Proportional, Integral, and Derivative

Contents

1	Introduction	2
1.1	Background	2
1.2	Problem	3
1.3	Purpose	4
1.4	Methodology	5
1.5	Delimitation	6
1.6	Outline	7
2	Theoretical Background	8
2.1	Fundamentals of Acoustics	8
2.1.1	The Sound Wave	9
2.1.2	Sound Pressure	11
2.1.3	Acoustics in the engine	12
2.1.4	Reducing Engine Noise	13
2.2	Engine	14
2.2.1	The Four-Stroke Cycle	14
2.2.2	Cylinders	15
2.2.3	HGR-Valve	18
2.2.4	Exhaust Brake Valve	18
2.3	The Optimization Problem	19
2.3.1	Objective Function	20
2.3.2	Constraints	21
2.3.3	Design Variables	22
2.4	Simulations	23
2.4.1	GT-Power	24
2.4.2	Optimization in GT-Power	27

2.4.3 Parallel Simulations, design of experiment (DoE)s	31
3 Method	32
3.1 Strategy	32
3.1.1 Baseline Simulation	32
3.1.2 Sub-problems	32
3.1.3 Optimization and DoEs	33
3.1.4 Evaluation	33
3.2 Setup	34
3.3 Results and analysis	35
4 The Procedure	36
4.1 Baseline Setup	36
4.1.1 Updated setup	37
4.2 First Optimization Simulations	37
4.2.1 Including all parameters	39
4.2.2 Design of Experiments	40
4.3 Results Analysis	40
4.4 The Optimal Solution	41
5 Results	42
5.1 Baseline	42
5.2 Optimization	44
5.2.1 First Optimization: Valve Lash, HGR-valve, Exhaust Brake Valve	44
5.2.2 The Complete Optimization Problem	51
5.3 Adjustments in the Model	56
5.4 The Optimal Design	59
6 Discussion and Conclusions	61
6.1 Discussion and Conclusions	61
6.1.1 Simulation Methods	61
6.1.2 Parameter Settings	65
6.2 Future Work	66
6.2.1 Component Settings	68
6.3 Final Words	69

List of Figures

1.1.1 Overall sound pressure level of different types of vehicles over vehicle speed. Heavy trucks are defined as vehicles with multiple-drive axles with a gross vehicle weight (GVW) typically over 12 000 kg. A vehicle for which the engine model in this study is suitable. [7]	3
2.1.1 Insertion loss for CAS1	13
2.2.1 Illustration of the four stroke operating cycle. [18, Chapter 1.3]	15
2.2.2 The volumetric efficiency over operating speed range for varied inlet (left) and exhaust (right) lash. [14, Chapter 6.6.4, Figure 13, 15]	17
2.3.1 A conceptual formulation of the optimization problem.	20
2.4.1 Illustration of the GT-Power model. Here the virtual microphone is marked in blue, whilst the parts at which constraints are measured are marked in red.	26
2.4.2 Illustration of the GT-Power model with the design variables' positions are marked in red.	26
2.4.3 The selection logic of the automatic selection option in the Design Optimizer of GT-Power [15, pp. 45].	30
3.2.1 TG21 limit and baseline brake-specific fuel consumption (BSFC) (numbers are scaled).	34
5.1.1 Sound pressure level with flow noise included and excluded respectively at baseline settings.	43
5.1.2 Output results at baseline settings together with given limits for maximum values.	43

LIST OF FIGURES

5.1.3 A zoomed in plot of Figure 5.1.2d showing the trampling of the turbo speed limit at baseline settings. The infringement is ongoing between 1670 and 1830 revolutions per minute (RPM) and is at most 1118 RPM over the limit (104000 RPM, i.e. 1.07 % above the limit).	44
5.2.1 Pareto front of the first multi-objective optimization showing the BSFC and the sound pressure level (SPL) including flow noise for each design generated.	45
5.2.2 Brake specific fuel consumption and sound pressure level including flow noise together with baseline levels as functions of the exhaust brake valve opening.	46
5.2.3 Sound pressure level including flow noise at 1500 RPM. Evolution over each design using the Design Optimizer.	47
5.2.4 Convergence of the design variables using the Design Optimizer for single optimization at 1500 RPM, minimizing the sound pressure level including flow noise.	48
5.2.5 Brake specific fuel consumption per design considered.	48
5.2.6 DoEs for the HGR valve being switched on and off. The two plots shows the acoustic output without and with flow noise included respectively. .	49
5.2.7 Acoustic output with and without flow noise included from a DoE simulation at 1500 RPM where inlet and exhaust valve lash are varied. The first design (Design 1) corresponds to 0 mm lash on both inlet and exhaust, thereafter the lash on either one or both valves (inlet and exhaust) are increased until the last design (Design 25) is simulated with 0.5 mm on both valves (inlet and exhaust).	49
5.2.8 The design with suggested optimal lash (blue) compared to the baseline setting (red). Note that the simulation is performed with the finer speed interval (step size 10 RPM) hence the less accurate shift for the HGR setting's interchange.	51
5.2.9 Brake specific fuel consumption for DoE simulation for the inlet and exhaust valve lash. The first design (Design 1) corresponds to 0 mm lash on both inlet and exhaust, thereafter the lash on either one or both valves (inlet and exhaust) are increased until the last design (Design 25) is simulated with 0.5 mm on both valves (inlet and exhaust).	52

LIST OF FIGURES

5.2.1 Brake specific fuel consumption for DoE simulation for the HGR-valve turned On and Off.	52
5.2.11 Average acoustic output and fuel consumption over the speeds simulated (1400-1700 RPM) for the complete optimization problem using the Design Optimizer.	53
5.2.12 Simulation of the brake specific fuel consumption with the exhaust cam timing angle as DoE varied between -90 to 0 degrees at 1500 RPM. Cylinder 1, 2, and 3 are varied in order to keep the run time down. Design 1 corresponds to -90 degrees on all three cylinders whilst Design 125 corresponds to 0 degrees on all three cylinders (as for the baseline settings).	54
5.2.13 DoE simulation for the fuel injection on cylinder 1, 2, and 3 varied $\pm 5\%$ for four speeds. Design 1 corresponds to -5 % gain on cylinder 1, 2, and 3, whereas Design 125 is simulated with +5 % gain on cylinder 1, 2, and 3.	54
5.2.14 Sound pressure level and brake specific fuel consumption over 751 designs considering fuel injection, lash, HGR-valve and exhaust brake valve. Evolution performed by the Design Optimizer towards settings to minimize acoustic output.	55
5.2.15 Sound pressure level and brake specific fuel consumption over 751 designs considering fuel injection, lash and HGR-valve.	56
5.3.1 Baseline and new cam lifting curves for the inlet and exhaust valves (left) and the absolute difference (right)	58
5.3.2 Acoustic output, SPL with and without flow noise included for the full speed simulation (600-2000 RPM with step size 10) comparing the results using baseline settings and the new cam lifting curve at optimal lash (0.35 mm on inlet and exhaust) and HGR-valve On (left) and Off (right).	58
5.3.3 Brake specific fuel consumption for the full speed simulation (600-2000 RPM with step size 10) comparing the results using the baseline settings and the new cam lifting curve at optimal lash settings (0.35 mm on inlet and exhaust, HGR-valve On and Off).	59
5.4.1 Difference in sound pressure level for the baseline and the optimal design suggested.	60

LIST OF FIGURES

A.o.1Optimization results for single optimization regarding valve lash and hot gas re-circulation (HGR)-valve.	72
A.o.2Multi-objective optimization results with the weighted-sum approach.	73
A.o.3Acoustic output (SPL including and excluding flow noise) from DoE simulations where inlet and exhaust valve lash are varied over different speeds.	73

List of Tables

2.1.1 Typical noise sources, together with an approximation of their corresponding SPL and sound pressure. [16]	11
2.2.1 Specifications of the Scania CBE1 engine	14
2.4.1 Terminology in GT-Suite [15, Chapter 1.1].	24
2.4.2 Specifics of the optimization algorithms in the Design Optimizer of GT-Power [15, pp. 46].	30
3.2.1 Limits for control output constituting the feasible region (TL21 is scaled due to confidentiality).	34
3.2.2 Baseline settings and initial ranges for the design variables.	35
4.2.1 Parameter settings for first optimization simulation.	38
4.2.2 Setup for the full optimization problem. (TL21 and TG21 constraints values are scaled).	40
5.2.1 Suggested optimal settings of the design variables considered in the single optimization using the Design Optimizer. The speed for the interchange in HGR-valve setting is taken from the DoE results.	47
5.2.2 Suggested optimal settings with the weighted sum approach at 1500 RPM. .	50
5.2.3 Suggested optimal settings for the complete problem (10 variables) at 1400-1700 RPM.	55
5.2.4 Suggested optimal settings for the viable problem (9 variables: valve lash, HGR-valve and fuel injection) at 1400-1700 RPM.	57
5.4.1 Suggested optimal settings for each parameter considered.	60
A.0.1 Suggested optimal settings with the weighted sum approach at 1500 RPM.	71

Chapter 1

Introduction

The goal of this study is to minimize the acoustic output from a compression ignition (CI) engine¹ without impairing overall performance. With the acoustic output as the objective function, an optimization problem is formulated with constraints defined in order to avoid deterioration of other performance parameters. The study is executed using simulations where the correlation between component settings and noise can be monitored. In order to find an optimal engine design regarding acoustic output, accurate methods are required. The methods used within this study are thus compared and evaluated in order to document their applicability to such problems.

This study is performed as a collaboration with Scania CV AB, hereinafter referred to as Scania.

1.1 Background

One of the biggest challenges in internal combustion (IC) engine development is noise reduction. Road traffic noise is one of the major sources to environmental noise and noise pollution, where heavy vehicles such as trucks and buses stands for the highest overall sound levels. As seen in Figure 1.1.1, the sound pressure level is significantly higher for trucks than for cars. [7]

Noise pollution is a growing concern and due to its harmfulness to human health, World Health Organisation (WHO) classes noise as an important public health issue.

¹A diesel engine in which the ignition is initiated by the elevated temperature caused by the mechanical compression [18, Chapter 1.8]

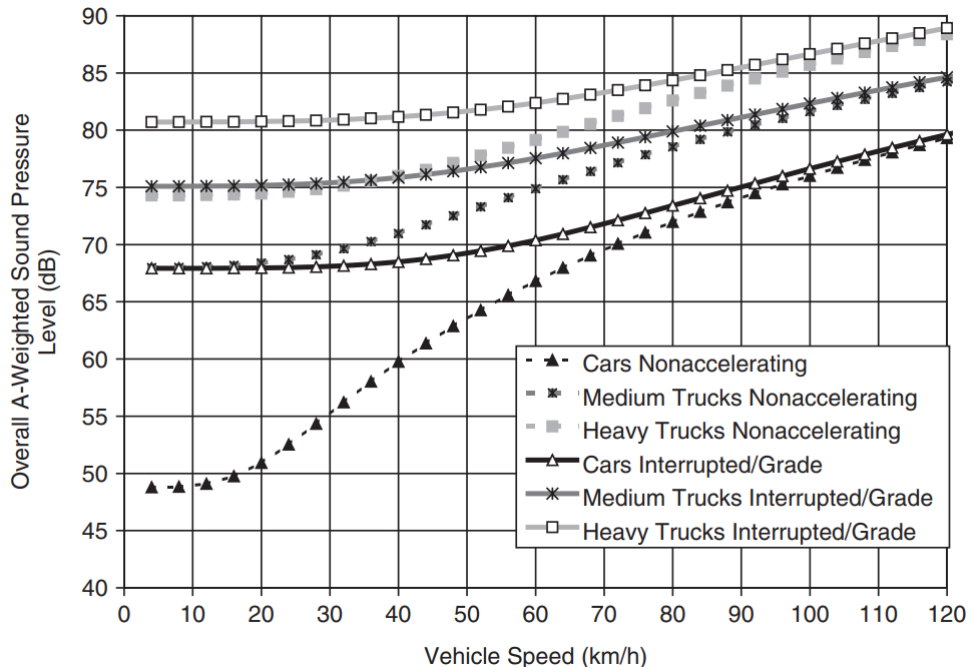


Figure 1.1.1: Overall sound pressure level of different types of vehicles over vehicle speed. Heavy trucks are defined as vehicles with multiple-drive axles with a GVW typically over 12 000 kg. A vehicle for which the engine model in this study is suitable. [7]

Noise exposure can directly injure the auditory system causing symptoms as hearing loss and tinnitus, but as a nonspecific stressor it may also have non-auditory effects on human health. [8] Especially following long time exposure, noise can cause psychological and physiological distress impairing the cardiovascular system. In turn, this may lead to coronary artery disease, arterial hypertension, stroke and heart failure [19]. Noise pollution is also affecting animals where their lifestyle may change with regard to communication, hunting and mating due to increasing noise levels in the environment. See [9] for example.

1.2 Problem

Within this study, the main goal is to minimize the engine's acoustic output over its operating speed range whilst taking other performance properties into consideration. This includes e.g. maximum performance, fuel consumption, air pollutant emissions, reliability and durability, maintenance requirements, and how these affect engine availability and operating costs. Some requirements are legislated whilst others must be satisfied in order to keep the products attractive on the market. The desired

performance requirements are often contradictory and a trade-off between them is necessary. The large number of components in engine design increases the difficulties. With the possibility of adjusting each component, at least to some extent, an almost infinitely large number of possible engine designs reveals. With the numerous performance requirements and all possible designs available, minimizing the acoustic output without impairing other performance parameters does not have an obvious solution. This is where the art of engineering truly comes to the fore. [18, Chapter 2.1]

Translating this into mathematics, an optimization problem arises for each speed within the operating speed range considered. The acoustic output is the objective function, the adjustable components assumes form of the design variables whilst the required performance parameters constitutes the constraints. To minimize noise over the full range of speed, the final objective will need to be a composite function, taking into account all the functions constituting the minimization over each speed.

The numerous acoustic sources and the complicated geometries of the IC engine generates a complex system over which sound propagates. The nature of acoustics intensifies the complexity even further. (A further presentation of the fundamentals of acoustics is found in Section 2.1). The operability and hardness of an optimization problem is not easily decided. It is considered to correlate to the complexity of the objective (or objectives if several) and constraints, together with how the feasible region is formed [1]. Here, the objective as well as some of the constraints are expected to be partial differential equations (PDE) and the number of design variables is considered large due to the variability of each component. In the same matter, the optimization problem is non-linear, thus the combined effects of variables and constraints must be considered. The problem attempted to be solved here can be considered very hard to solve mathematically.

1.3 Purpose

Due to the effect of noise pollution on humans and wild life, minimizing the acoustic output is highly prioritized within IC engine design. The Scania diesel engine CBE1 used in this study is of its final stage of development. In order to improve acoustic performance, further investigation of the acoustic output is necessary. In order to do this, the methods for acoustic simulations has to be accurate. One of the main

goals of this project is therefore to evaluate and ensure the quality of the methods available.

The optimization is performed over a full operating speed range, 600 to 2000 RPM. The main target for the minimization lies within the range 1400 to 1700 RPM, since it is the range over which legislated noise level tests are performed in the EU[21]. The CBE1 is approved for these tests already, but further improvements are expected. In the USA, legislation tests are performed above 2000 RPM. This speed is thus considered the second most important target for this study if the CBE1 would to be launched on the U.S. market as well.

In order to minimize the noise levels without impairing performance, it is of great importance to understand how control of the components influence the acoustic output. The study aims to give rise to this issue to enable well-founded decisions in further development of this model.

1.4 Methodology

In order to circumvent the mathematical complexity of the problem, a simulation software is used throughout this study. As already recognized (Section 1.2), the number of performance requirements and components to adjust must be limited to enable qualitative simulations. Hence, only a few performance parameters are selected together with a choice of components and their possible settings. Initially a literature study is made in order to find results of previous studies in the field and to understand possible sources of noise in IC engines. An optimization problem is formulated conceptually for the selected components and a feasible region is formed by the constraints. For the given model, a baseline simulation is performed and set as target for the project.

In an initial phase, the optimization is focused on the settings of the components. As optimal settings are found, consideration of geometrical modifications of the components are investigated instead. These processes will hereinafter be named control optimization and hardware optimization respectively.

The software used performs optimization as well as parallel simulations to compare different component settings. Both functionalities are used and evaluated throughout this study. Due to the complexity of the optimization problem, the applicability of the

the optimization tool provided is not guaranteed. Therefore, it is tried out on smaller problems initially and from the results obtained, a strategy for the progression of the project is formed simultaneously. If the results are not satisfactory, the parallel design option is used instead to complete the investigation.

The results from both methods are used in order to understand how different performance parameters are affected by the settings and what the trade-off is when minimizing the acoustic output. Despite the non-linearity of the optimization problem, an iterative process is executed where results from initial runs are being used to decrease the complexity of the full range problem. This process is developed with continuous consultancy of the experienced engineers at Scania to give valuable inputs on viability, accuracy and suggested continuation.

1.5 Delimitation

In this study, the engine and the exhaust system are studied in order to minimize the acoustic output without impairing the effect.

This study is limited to simulate the SPL from the engine and the exhaust system exclusively. The acoustic output is measured at the absolute outlet of the exhaust system, hence the total SPL is simulated regardless of its source. The exhaust system of this model already includes a well performing muffler. The muffler reduces the exhaust sound, especially at certain frequencies. No adjustments or investigation of it will be performed within this study, as it focuses on minimizing the generation of noise rather than silencing it.

The desired performance requirements are not all considered within this study in order to keep the optimization manageable. Instead, a selection of outputs of the simulations are selected to keep control of overall performance. Other performance requirements may be considered in the discussion as the results are being analyzed. The number of components considered is also limited. The selected components are suggested to have impact on the noise level to some extent, whilst they are considered to be adjustable without impairing vital performance. The study is executed with a specific engine. If the result is applicable to other, similar engines is not investigated in detail.

The study does not perform a mathematical solution of the optimization problem that arises. Nor is an explicit mathematical formulation presented. This is due to the

complexity of the problem and the fact that a simulation software is used to investigate the acoustic behaviour.

1.6 Outline

The study covers effects on acoustic and performance output from control and hardware tuning as well as the performance effects of noise minimization. In order to investigate the sound levels from the engine, basic knowledge of acoustics, mechanics and engine design is required. This is specified in Section 2.1 and 2.2. Details of the mathematical approach can be seen in Section 2.3. The research is being conducted using the simulation software GT-Power. A closer presentation of it and its functionalities is seen in Section 2.4.1, whilst specifics of the setup is found in Section 3.2 as well as in chapter 4. The overall procedure and the approach to perform this study is presented in chapter 3 and 4. Further on, results are announced in chapter 5 which in the succeeding chapter, (chapter 6) are evaluated and analyzed together with suggestions on future work.

Chapter 2

Theoretical Background

To handle the problem from a mathematical point of view, understanding of acoustic wave theory and basic knowledge about the engine is required. This is presented in this Section together with an introduction to the simulation software used.

From the initial literature study, no previous studies are found where simulation methods for acoustic optimization are developed for the exhaust system with a similar approach as here. This is just as expected, thus the purpose of this project. Nevertheless, due to the complexity of acoustics and the importance of noise minimization, engine noise is an extensive research field. Despite contributing directly to the actual work of this study, many interesting papers are found which can contribute to the work by the general use of optimization algorithms in engine noise minimization. See [3] for an example.

2.1 Fundamentals of Acoustics

Sound is the propagation of changes in air pressure and hearing is the detection of such pressure changes by the ear. The human sense of hearing corresponds to frequencies in between 20 Hz to 20 kHz, with the highest sensitivity within 100 Hz to 10 kHz, a range which corresponds well to human speech. [22, pp. 139]

2.1.1 The Sound Wave

The sound wave equation can be derived from the Navier-Stokes equations for density ρ , pressure p , and particle speed v :

$$\begin{cases} \frac{\partial \rho}{\partial t} + \frac{\partial}{\partial x}(\rho v) = 0, \\ \rho \frac{\partial v}{\partial t} + \rho v \frac{\partial v}{\partial x} + \frac{\partial p}{\partial x} = 0, \\ p = K\rho^\gamma. \end{cases} \quad (2.1)$$

The first equation is the law of mass conservation, the second arises from the equation of gaseous motion and the third is the gas law for adiabatic ¹ processes. K and γ are constants according to the medium the wave travels through. Sound is represented by perturbations in the air pressure, hence

$$\tilde{\rho} = \frac{\rho}{\rho_0}, \quad \tilde{p} = \frac{p}{p_0} - 1, \quad \tilde{v} = \frac{v}{v_0} \quad (2.2)$$

are introduced, where ρ_0 and p_0 represents the state of equilibrium. At the state of equilibrium, $v = 0$, and $v_0 = \sqrt{\gamma p_0 / \rho_0}$ will appear to be the speed of propagation. The perturbations can be considered small, thus insertion of (2.2) into (2.1), together with linearization and the assumption that $v \ll v_0$,

$$\begin{cases} \frac{1}{\gamma} \frac{\partial \tilde{p}}{\partial t} + v_0 \frac{\partial \tilde{v}}{\partial x} = 0, \\ v_0 \frac{\partial \tilde{v}}{\partial t} + \frac{p_0}{\rho_0} \frac{\partial \tilde{p}}{\partial x} = 0, \\ \tilde{p} = \gamma \tilde{\rho} \end{cases} \quad (2.3)$$

is obtained. The first two equations of (2.3) consolidates a system of linear PDEs, thus the wave equation for a one dimensional sound wave can be derived for the pressure \tilde{p} :

$$\frac{\partial^2 \tilde{p}}{\partial t^2} - \frac{\gamma p_0}{\rho_0} \frac{\partial^2 \tilde{p}}{\partial x^2} = \frac{\partial^2 \tilde{p}}{\partial t^2} - v_0^2 \frac{\partial^2 \tilde{p}}{\partial x^2} = 0. \quad (2.4)$$

This can be derived similarly for $\tilde{\rho}$ and \tilde{v} as well. In a more general form, for the atmospheric pressure, p , equation 2.4 is written

$$\frac{\partial^2 p}{\partial t^2} - c^2 \frac{\partial^2 p}{\partial x^2} = 0. \quad (2.5)$$

¹A thermodynamic process which involves no change in entropy, the physical property associated with a state of disorder. [2]

Equation 2.5 describes the sound wave in one dimension, a longitudinal wave motion in the x -direction with velocity c . [25]

The general solution of (2.5) is:

$$p(x, t) = f_1(x - ct) + f_2(x + ct). \quad (2.6)$$

The functions $f_1(x - ct)$ and $f_2(x + ct)$ represents two independent waves traveling in the positive and negative x -directions respectively, both with velocity c . f_1 and f_2 are completely general continuous functions of their arguments. $f_1(x - ct)$ represents a wave of arbitrary spatial shape $f_1(x - x_0)$ or of arbitrary time behaviour $f_1(ct_0 - ct)$ propagating in the positive x -direction. Similarly for $f_2(x + ct)$ for propagation in the negative x -direction. In the frequency domain, a solution to equation (2.5) will be of the form

$$p(x, t) = Ae^{-j kx} e^{j \omega t} + Be^{j kx} e^{-j \omega t}, \quad (2.7)$$

where $k = \omega/c$ for the angular frequency ω and the A and B terms represent waves traveling to the right and the left respectively. For a wave traveling in the positive x -direction, $B = 0$ and $A = 1$ in (2.7), hence

$$p = e^{-j kx} e^{-j \omega t} \rightarrow \cos(-kx + \omega t), \quad (2.8)$$

where the second form is the real part of the first. Let u be the velocity of the acoustic fluid, or particle velocity. Then,

$$p = \rho c u. \quad (2.9)$$

From this the wave impedance or the specific acoustic impedance, z , can be defined:

$$z = \frac{p}{u} = \rho c. \quad (2.10)$$

The wave impedance describes the (acoustic) pressure over a unit of length in units of $[\text{Pa m}^{-1}]$.

The theory of the sound wave in one dimension described above can be converted into three dimensions without loss of generality. In three dimension, the Laplace operator, $\Delta : \mapsto \frac{\partial^2 p}{\partial x^2} + \frac{\partial^2 p}{\partial y^2} + \frac{\partial^2 p}{\partial z^2}$, operates on the acoustic pressure $p(x, y, z, t)$, hence the three

dimensional sound wave equation is:

$$\frac{\partial^2 p}{\partial t^2} - c^2 \Delta p = 0, \quad (2.11)$$

for the speed of propagation c . [22, Chapter 6.1]

2.1.2 Sound Pressure

The most commonly used indicator or the acoustic wave strength is the sound pressure level, L_p . For an acoustic pressure p , L_p is defined

$$L_p = 20 \log_{10} \left(\frac{p}{p_0} \right), \quad (2.12)$$

measured in decibels (dB) above the reference pressure p_0 . p_0 is by convention set to $20 \mu\text{Pa}$, the approximate root mean squared (RMS) threshold for human hearing in its most sensitive range. Hence, the average human range of hearing starts at 0 dB. A threshold of pain for humans is referenced at 120 dB. [22, Chapter 6.3]

Table 2.1.1 gives some examples of typical sound sources and their approximate corresponding pressure and SPL.

Typical noise source	SPL [dB]	Sound pressure [Pa]
Average hearing threshold	0	0.00002
Whispering	45	0.004
Normal conversation at 1 m	60	0.02
Passenger car, 80 km/h at 15 m	65	0.04
Diesel truck, 70 km/h at 15 m	75	0.1
Teenage rock and roll band	110	6
Firearms	160	2000
Large military weapons	180	20 000

Table 2.1.1: Typical noise sources, together with an approximation of their corresponding SPL and sound pressure. [16]

Typically, a noise signal consists of several harmonics, assumed to be incoherent. A mean-squared sound pressure level from n different sources L_1, L_2, \dots, L_n is thus given

by

$$L_{\Sigma} = 10 \log_{10} \left(10^{\frac{L_1}{10}} + 10^{\frac{L_2}{10}} + \dots + 10^{\frac{L_n}{10}} \right) \text{dB.} \quad (2.13)$$

[10]

2.1.3 Acoustics in the engine

Motor vehicle noise is generated by several sources, which for the exterior motor vehicle can be separated into three main categories: power train, tire-pavement, and aerodynamic noise. The power train noise includes all sources associated with vehicle propulsion. This includes the exhaust outlet noise as well as noise from the engine, the cooling fan, transmission and gears, mechanical vibrations on the engine components, etc. [7]

In this study, the noise generated by the engine itself as well as the noise from the exhaust system are investigated. These type of acoustics can be separated into two main types: combustion noise and flow noise. Combustion noise is, as the name suggests, the noise of the combustion in each cylinder. Combustion noise is generated by the pressure wave itself and the mechanically generated noise due to vibrations or oscillating forces on, or amongst mechanical parts. Combustion noise is higher for CI engines than for spark ignition (SI) engines² due to the fact that the combustion is more sudden which causes the cylinder pressure to rise more abruptly. [18, Chapter 15.35]

Flow noise occurs in all parts of the engine where gaseous flows passes and is generated as the gaseous air or air-fuel mixtures flowing through the system. In the exhaust system it originates from the exhaust blow-down process of each cylinder as the pressure waves passing through the exhaust system and entering the atmosphere. Similarly, on the intake side, flow noise originates from the pressure wave generated by the periodic induction process in the cylinder. The velocity and flow rate is what impacts the SPL of the flow noise the most. Due to the periodic opening of the exhaust valves after each combustion, the exhaust noise dominates the aerodynamic noise and will furthermore be concentrated at specific frequencies. These frequencies, or engine orders, are the main targets in exhaust muffler development. [18, Chapter 15.35] [13, Chapter 1.2.2]

²IC engines where the combustion process of the air-fuel mixture is ignited by a spark plug.

2.1.4 Reducing Engine Noise

According to equation 2.13, a reduction of the largest source of noise (which is the engine itself out of the noise sources investigated here) will have the greatest impact on the total SPL reduction and is thus the main target.

In engine noise reduction, the exhaust muffler plays an important role and a major part of the research in the acoustic field at Scania is focused on improving the exhaust muffler performance. The CBE1 engine is equipped with a Scania muffler named CAS1 which is not being part of the investigation within this project. Nevertheless, it is important to understand how it operates in order to analyze the result from the acoustic output correctly.

The effect of the implementation of a muffler can be computed in dB via the insertion loss IL ,

$$IL = 10\log_{10} \left(\frac{P_T}{P_R} \right). \quad (2.14)$$

Here, P_T and P_R are the pressures before and after insertion of the muffler respectively. The insertion loss for the CAS1 muffler over frequency is shown in Figure 2.1.1. It is seen that the muffler's insertion loss is high over approximately 100 Hz, which corresponds to 2000 RPM, the upper limit of the operating speed range for this study.

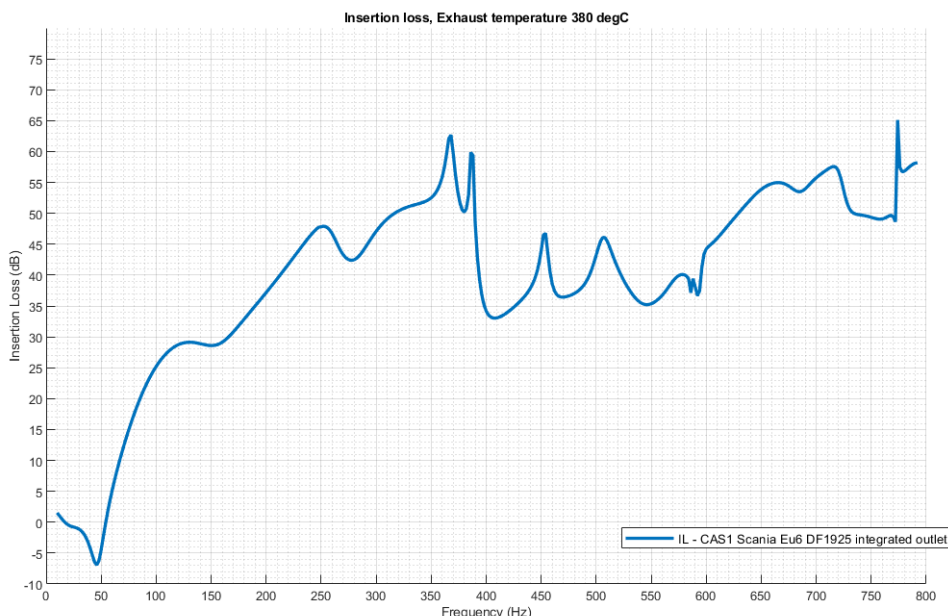


Figure 2.1.1: Insertion loss for CAS1

To convert frequencies to speed, the engine's design must be taken into consideration. The speed is the number of RPMs that the shaft, to which each cylinder is attached, performs per minute. In a six-cylinder engine, the cylinders moves in pairs, hence the engine performs $6/2 = 3$ revolutions per minute. For a given frequency f , the corresponding speed is thus $(60/3)f = 20f$ RPM.

2.2 Engine

This study is executed using a four stroke, six cylinder CI engine. The model is developed by Scania and is in its final stages of design. The main specifications of the engine are summarized in Table 2.2.1. The model name CBE1 will be used throughout this report when referring to this specific model.

In this section, the four stroke cycle is described. A general description of the different components investigated within this study is also included.

Engine type	Four stroke
Ignition	Compression ignition (CI)
Fuel	Diesel
Cylinders	Straight, six cylinders
Stroke volume	12.74 liters
Max. effect	560 hp (412 kW) at 1800 RPM
Max. torque	2800 Nm at 900-1400 RPM

Table 2.2.1: Specifications of the Scania CBE1 engine

2.2.1 The Four-Stroke Cycle

The CBE1 operates by a four-stroke cycle, where each cylinder requires four strokes of its piston to complete the sequence of events that produces one power stroke. The top-most and the bottom-most positions are named top center (TC) and bottom center (BC) respectively. The process is illustrated in Figure 2.2.1. Starting from TC the four strokes are as follows: [18, Chapter 1.3]

1. Intake Stroke

The inlet valve opens and allows fresh air to be drawn into the cylinder as the piston moves from TC. Valve closes again as piston arrives at BC.

2. Compression Stroke

As the piston moves back from BC to TC with all valves closed, the air in the cylinder is compressed to a small fraction of its initial volume. As the piston approaches TC again, diesel is injected in a short pulse through several nozzle holes. Combustion is initiated as the high pressure causes ignition of the air-fuel mixture gas.

3. Power Stroke (Expansion Stroke)

From the explosion, the piston is pushed by the high-temperature, high-pressure gases from TC to BC. This motion forces the crank to rotate. About five times more work is done on the piston during this stroke as during the compression stroke. The exhaust valve opens as the piston approaches BC which initiates the exhaust process as cylinder pressure drops.

4. Exhaust Stroke

With the exhaust valve open, the remaining burned gases exit the cylinder. Initially this is caused by the significantly higher pressure in the cylinder than in the exhaust system and the remaining gases will be swept away as the piston again moves from BC to TC. As the piston reaches TC, the exhaust valve closes and the inlet valve opens, initiating a new cycle to begin.

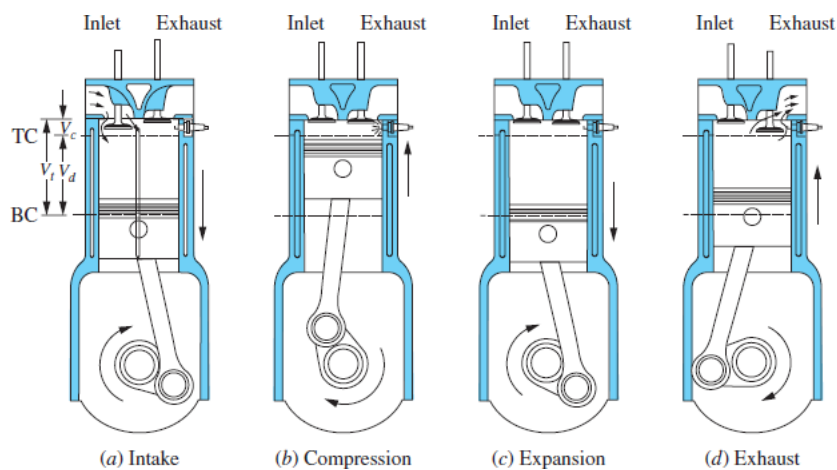


Figure 2.2.1: Illustration of the four stroke operating cycle. [18, Chapter 1.3]

2.2.2 Cylinders

The power produced each stroke corresponds to the size of the explosion inside the cylinder. A bigger volume of air compressed and more fuel burnt will generate a bigger explosion. Thus, a primal design goal for the cylinders to maximize power generation

is to inject enough fuel and induce as much air as possible at full load at any given speed. This is in order to maximize the volume of air-fuel mixture to be ignited. Nevertheless, a bigger explosion requires more fuel and will generate more noise. This is the justification for investigating the cylinders in this project. [18, Chapter 1.8]

The acoustic output is investigated with respect to three different component settings considering cylinder design: fuel injection (control optimization), valve lash (control optimization) and cam timing angle (hardware optimization) which controls when the valves opens and closes. These will be described in more detail below.

The intake and exhaust system governs the flow of gases into and out of the cylinders respectively. In the CBE1, each cylinder has two inlet and two exhaust valves. Their design and movement are important components in order to control the amount of fresh air introduced and how much hot, burned gas is allowed out of the cylinder within each stroke. For this project, the valve functionalities investigated are valve lash and cam timing angle.

The cylinder's air flow capability, also called its volumetric efficiency, is defined

$$\eta_v = \frac{m_a}{\rho_{a,i} V_d}. \quad (2.15)$$

m_a is the mass of air inducted into the cylinder per cycle, V_d is the displacement volume of the piston and $\rho_{a,0}$ is the air density, usually evaluated at atmospheric conditions. If written as in equation (2.15), η_v is the overall volumetric efficiency. If instead the volumetric efficiency of a specific cylinder, the intake port or the valve alone is of interest, $\rho_{a,i}$ is used for index i corresponding to the component selected. [18, Chapter 2.10]

Valve Lash

Valve lash is the mechanical clearance in the valve train between camshaft and valve in an IC engine. Figure 2.2.2a and 2.2.2 shows a general volumetric efficiency of different intake and exhaust lash respectively. [14]

A clearance too large will cause the engine to lose compression which impairs performance. A clearance too narrow will instead slow down the valve closing and cause ware on the mechanical parts which in turn may overheat the engine. The clearance is covered with a thin oil film to lubricate the parts and in order to reduce

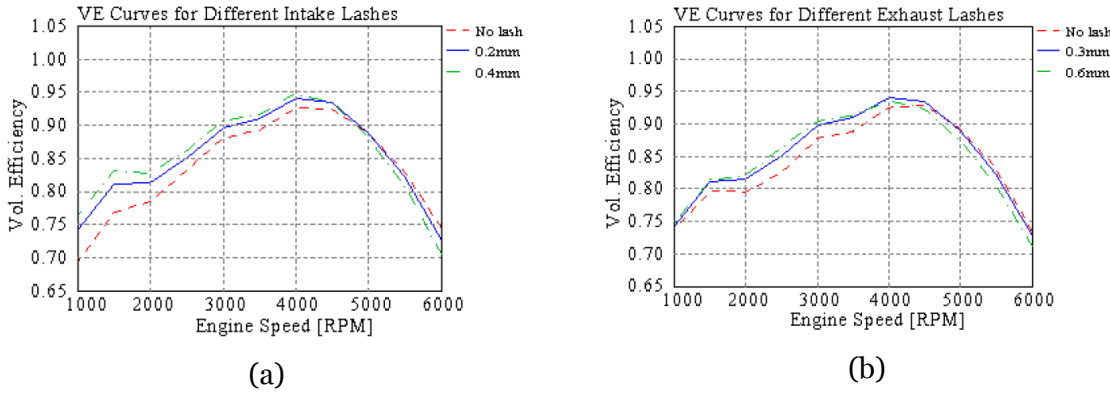


Figure 2.2.2: The volumetric efficiency over operating speed range for varied inlet (left) and exhaust (right) lash. [14, Chapter 6.6.4, Figure 13, 15]

friction. The size of the clearance should therefore be small enough to allow this film of oil to be intact, yet large enough to allow this oil film to lubricate the components. Typical values of lash is 0.0 to 0.9 mm, but since the materials will expand as the temperature in the engine increases, valve lash is not easily measured and is therefore also hard to adjust accurately. [14, Chapter 6.6.4]

Cam Timing Angle

The valves' opening and closing controls the flow of gaseous throughout the system. Their motion is determined by the shape of the cam movement throughout the stroke cycle. The valves motion is controlled to open and close at a specific cam angle, here referred to as the cam timing angle. The cam rotates from zero to 360 degrees each stroke, starting from TC. Following the four stroke cycle, the inlet valves should open sometime during the intake stroke, 0 to 90 degrees and the exhaust valves at 270 to 360 degrees (or -90 to 0 degrees). [18, Chapter 6.3]

Fuel Injection

The fuel injectors introduces fuel into the combustion chamber. The CBE1 is a direct-injection diesel engine, which allows for multiple pulse injections of periodic pressure or mass flow rate profiles [14, Chapter 2.7.4]. The amount of fuel required for each speed in the operating range is computed by GT-Power in order to maintain a specific moment on the crankshaft. The system computes the required amount using a Proportional, Integral, and Derivative (PID)-regulator which computes the input signal $u(t)$ (here, the amount of fuel required in grams) based on the difference between

desired and real output, $e(t) = r(t) - y(t)$ as

$$u(t) = K_P e(t) + K_I \int_0^t e(\tau) d\tau + K_D \frac{d}{dt} e(t). \quad (2.16)$$

In order to understand the correlation between acoustics and the amount of fuel injected, simulations are run where the amount of fuel injected is manipulated, i.e. when the PID-regulator is switched off. [11]

The fuel consumption is considered one of the most important performance parameters and for the CBE1, fuel saving is already more than 8 % compared to Scania's current engine range [23]. Due to the high fuel efficiency, changing the amount of fuel injected is in reality not viable. Nevertheless, it is still of interest to understand the correlation between amount of fuel injected and acoustic output. Rather than finding the amount of fuel which generates the lowest acoustic output, the goal for this investigation is instead to make the trade-off between them visible.

2.2.3 HGR-Valve

The HGR-valve allows hot exhaust gases to be transferred back to the intake. This is an efficient method for heating up a cold engine, but more importantly, the re-circulation of the exhaust gases decreases the oxygen rate of the intake gases. With a lower oxygen rate on the intake, nitrogen oxide (NO_x) emission levels are decreased. This is the main purpose of any exhaust gas re-circulation (EGR) system, but in most applications the gases are cooled down before re-entering the cylinders in order to minimize the volume of the air induced by the intake valves. This is not the case for the CBE1, where the hot gases re-circulates without cooling. The HGR-valve is either completely closed or fully open and due to the additional flow, the system is expected to generate higher acoustic output with the valve open. [18, Chapter 11.1]

2.2.4 Exhaust Brake Valve

The exhaust brake valve is part of the exhaust system and controls how much of the exhaust gases are allowed out of the system. Throttling the valve creates a back-pressure in the exhaust system as the flow is not allowed to pass. This causes pressure to build up backwards through the system, slowing the cylinder down. This is used in order to give extra brake power in combination with fuel restriction (i.e. not giving

more gas) since the truck brakes without using the brake pedal. [26]

For the purpose of this project, the simulations are always run with full load. The full load seeks to simulate the truck as it uses its full power, for example heavily loaded travelling up a steep hill. Thus, throttling the exhaust brake vault whilst maintaining full load, a higher fuel consumption as well as increased noise levels are expected. A simulation with full load and throttled exhaust brake is therefore not realistic, but the investigation may still provide interesting result for the acoustic dependency.

2.3 The Optimization Problem

Due to the complexity of the problem and the fact that a simulation software is used, the problem is not formulated mathematically as concluded already in Section 1. Instead, a conceptual formulation is used to enable mathematical analysis of the result in order to understand how the output is affected by the component settings. The conceptual problem formulation is assumed to take form of a standard formulation of a general nonlinear optimization problem:

$$\begin{cases} \underset{\vec{x}}{\text{minimize}} & f(\vec{x}) \\ \text{subject to} & \vec{x} \in X. \end{cases} \quad (2.17)$$

$f : \mathbb{R}^n \rightarrow \mathbb{R}$ is the objective function, $\vec{x} \in \mathbb{R}^n$ is the vector of variables and X is defined by a set of given functions $g_1(\vec{x}), g_2(\vec{x}), \dots, g_m(\vec{x})$ from \mathbb{R}^n to \mathbb{R} which constitutes the feasible set of the problem, i.e. $X = \{\vec{x} \in \mathbb{R}^n : g_i(\vec{x}) \leq 0, i = 1, 2, \dots, m\}$. f and g_1, \dots, g_m are assumed to be continuously differentiable and at least one of them is nonlinear.

In order to optimize for several performance parameters simultaneously, a multi-objective optimization problem is considered:

$$\begin{cases} \underset{\vec{x}}{\text{minimize}} & f_1(\vec{x}), f_2(\vec{x}), \dots, f_k(\vec{x}) \\ \text{subject to} & \vec{x} \in X. \end{cases} \quad (2.18)$$

Here, the definitions are similar as (2.17), but with the difference that there are k objective functions to be minimized. multi-objective optimization problems can in some senses allow a degree of freedom in the modelling, but it often comes at the

expense of making them more difficult to solve. Due to the different, often conflicting objectives, no single solution exists that simultaneously optimizes each objective. Instead, a set of solutions, the trade-off surface, is given. The solutions within this set are called Pareto solutions. Without additional subjective preference information, these solutions are considered equally good, thus the trade-off between them must be taken into account when picking a singular optimal solution from this set. [5]

The built-in optimizer used throughout this study handles both single- and multi-objective problems. Both functionalities will be examined within this study in order to evaluate their utility and compare results from the different approaches.

With the formal definitions (2.17) and (2.18) as a starting point, the conceptual formulation for the optimization problem(-s) considered in this study is presented as a hierarchy model in Figure 2.3.1.

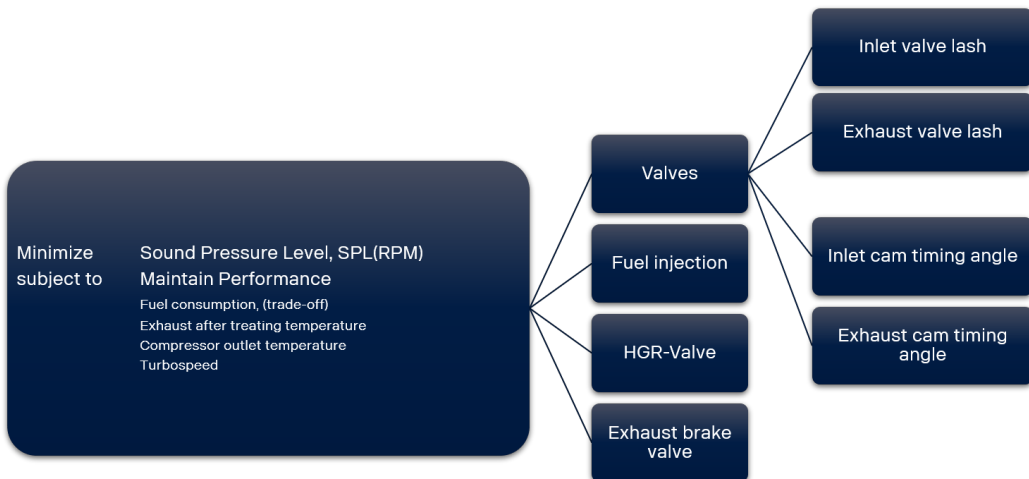


Figure 2.3.1: A conceptual formulation of the optimization problem.

2.3.1 Objective Function

With the aim to minimize the acoustic levels over a given range of operating speed, the objective function will be some acoustic output for each speed over this range. Thus, for each speed within the range, an individual optimization problem will arise. In order to minimize the overall sound pressure level, a weighted sum over the range can be considered with higher weights on speeds that are considered to be more important.

From the simulation software used, the acoustic output considered as the objective is the SPL in dB for all speeds in the operating speed range. The acoustic level is measured

at the exhaust outlet and is given either with or without flow noise which allows further analysis of which type of noise is affected by the component changes.

For the other performance parameters considered, the fuel consumption is prioritized. The fuel consumption can be simulated as the BSFC (see below, Section 2.3.2) and is in some cases considered a second objective to emphasize its importance within this study.

2.3.2 Constraints

In order to control that performance is preserved, some general physical properties are set as constraints to the problem. These are outputs from the simulations which together forms the feasible region of the problem. The fuel consumption (BSFC) is not constrained by an upper limit, but is examined separately as a result output for each simulation because of its great importance. Fuel consumption is measured as BSFC in milligrams of fuel injected per second, r , over the power produced, P ,

$$BSFC = \frac{r}{P}, \quad \left[\frac{mg/s}{W} \right] = \left[\frac{g}{kWh} \right]. \quad (2.19)$$

In addition to fuel consumption, three constraints are defined which together constitutes a region where the engine is known to operate well. These are:

- **Turbospeed:** The speed of the turbo charger, [RPM],
- **TL21:** Compressor outlet temperature. Temperature measured between the compressor and the cooling system, [C],
- **TG21:** Exhaust After-treating temperature. Temperature measured just after the exhaust brake, [C].

The names of these parameters are taken from the model setup (see Figure 2.4.1). Specific values are given in Section 3.2.

Despite the fact that these constraints encloses a region where the engine operates well, all desired performance parameters are not being considered. Nitrogen oxide (NO_x) emission, cost efficiency and sustainability are examples of parameters which are not explicitly included. Nevertheless, their importance should not be underestimated and they will be considered when discussing the simulation results in Section 6. This can be seen as a form of relaxation of the problem in order to reduce the number of constraints.

Within the scope of this study, the main goal is to present a design with suggested changes to minimize acoustic levels considering the constraints listed above. The final analysis and decision basis is submitted to the experts of the field.

2.3.3 Design Variables

The number of components that constitutes the CBE1 and their ability to be adjusted or even exchanged, creates an almost infinite number of design variables. Within the framework of this project, some interesting components are selected. Initially this includes control optimization, or tuning of already existing components to thereafter proceed on hardware optimization where larger changes to the geometry or exchange of components are investigated.

The variables could be considered discrete since they consist of physical units such as length, mass, temperature or angle and the actual settings cannot be made with infinitely high precision. From an optimization point of view, this will not make the problem less complex, but rather the opposite. The Design Optimizer will thus consider all variables continuous except for the HGR-valve variable which is explicitly given as discrete as it can only be turned on or off. For the DoE simulations, only the minimum and maximum limits are given as well as the number of steps considered, thus a type of discretization is considered here.

The design variables and a brief description of how they can be adjusted is presented here. A description of their functionalities were given in Section 2.2.2 to 2.2.4.

- **Valve lash**, Control Optimization:

The valve lash is considered the same for all inlet valves and all outlet valves respectively. In theory, each valve could be handled individually, which would generate 12 intake and 12 exhaust valves to optimize over. Nevertheless, the effect of lash is considered to be equal for all cylinders on the intake and the exhaust side respectively, thus only two variables are considered where the intake and the exhaust sides are controlled jointly:

- Inlet lash, one variable.
- Exhaust lash, one variable.

- **Fuel injection**, Control Optimization:

Manipulated amount of fuel given in each injection. The fuel injected will be

varied $\pm 5\%$ with the required amount as a reference. The extra fuel can be distributed individually for all six cylinders, yielding up to six variables. In opposite to the lash, some effect of individual injections to each cylinder could be expected due to the combustion sound which varies with different amount of fuel. Thus, the fuel injection can be considered as one or up to six variables.

- Additional fuel to injector of cylinder 1,...,6, up to 6 variables.
- **HGR-valve**, Control Optimization:
The exhaust gas re-circulation will automatically vary at different operating temperatures for the actual engine. Here, the opening and closing of the HGR-valve is controlled manually in order to investigate the acoustic effects. The HGR-valve can either be turned On or turned Off, hence considered a binary variable.
 - HGR On/Off, one variable (binary).
- **Exhaust brake valve**, Control Optimization:
The percentage of throttling of the valve.
 - Exhaust brake valve opening, one variable.
- **Cam timing angle**, Hardware Optimization:
The cam timing angle is investigated for the intake and exhaust sides of each cylinder separately. The two inlet valves at each cylinder as well as the two at the exhaust side are jointly tuned. Up to 12 variables may be considered on each side for all six cylinders. Here, each pair of cylinders moving together each stroke will be jointly tuned, yielding 3 variables on each side:
 - Cam timing angle on the intake side of cylinder 1 and 6, 2 and 5, 3 and 4, 3 variables.
 - Cam timing angle on the exhaust side of cylinder 1 and 6, 2 and 5, 3 and 4, 3 variables.

2.4 Simulations

As already presented, this project is performed using a simulation software, GT-Power, which is introduced in more detail here. By the thorough tests and simulations already performed on the CBE1 throughout its development, a large amount of output data

Case	A stand-alone simulation representing an operating point. Within this project, there is one case for each speed within the operating range [600-2000] RPM.
RLT	A model output, short for “Result”.
CaseRLT	The final RLT value at the end of a case simulation.
DoE	Design of experiment (DoE), a parallel design simulation where one or more parameters are varied between pre-defined values for each case throughout the simulation. (Further described in Section 2.4.3)
Factor	An independent variable or model input, used in the context of optimization or DoE.
Response	A dependent variable or model output, used in the context of optimization or DoE.
Design	A particular combination of factors and their corresponding responses considered in the optimization runs.

Table 2.4.1: Terminology in GT-Suite [15, Chapter 1.1].

is available. This output data creates a map of information to describe the engine’s function and behaviour which in turn improves accuracy of further simulations. The simulations performed throughout this project are considered to have a very high accuracy and validity for the actual acoustic output.

2.4.1 GT-Power

GT-Power is a simulation software for the transportation industry within the GT-Suite developed by Gamma Technologies. Models are built up by a set of one dimensional components which simulates the physics of several properties, acoustic flow included. [12] In order to simulate the acoustic output, one (or more) virtual microphone(-s) can be placed at different locations of the simulation model depending on the purpose of the investigation. Within this study, one microphone is used, which is placed at the outermost orifice of the exhaust system. Setup specifications are found in Section 3.2.

Terminology in GT-Power

Terminology in GT-Suite is presented in Table 2.4.1 in order to follow the discussion and relate setup and results.

Acoustic Simulations in GT-Power

Acoustics are simulated by converting time domain signals, such as sound pressure waves, to the frequency domain and vice versa using fast Fourier transform (FFT), further described below. [13, Chapter 1.1] GT-Power solves the one dimensional Navier-Stokes equations (2.1). To accurately capture plane waves travelling in all directions, the simulated flow is split into different directions together with a three dimensional discretization. This way, plane waves moving in three directions can be tracked by the one dimensional solution. For the frequency range investigated here, plane waves dominates and the accuracy of the simulations are thus considered very high over this range. The pressure wave simulated result in noise propagating from the intake to exhaust orifices of the engine. [13, Chapter 1.1.1]

GT-Power provides a microphone (AcoustExtMicrophone) to predict the free field SPL. In this study, one microphone is placed at the outermost orifice of the exhaust system and does not include ground and drive-by effects. Flow noise is included and can be separated in the output data (SPL or SPL plus Flow). By treating the orifice as a simple pulsating monopole, the pressure, P , at the free-field location of the microphone is computed by transforming the instantaneous velocity at the orifice, u by the following equation.

$$P = \frac{\rho S}{\text{const} \cdot \pi r} \frac{d}{dt} \left[u(t - \frac{r}{c}) \right], \quad (2.20)$$

where ρ is the density of the free medium, S , the cross sectional area of the orifice, r , the distance between microphone and orifice, t , time and c the speed of sound in the free field. The constant, const is 4 for spherical radiation and $2\sqrt{2}$ for hemispherical radiation.

Figure 2.4.1 and 2.4.2 illustrates the CBE1 engine in GT-Power. The parts of interest for this study are marked specifically.

Fast Fourier Transforms (FFT)

A FFT is an algorithm that computes the discrete Fourier transform (DFT) of a sequence or its inverse. The DFT is a matrix-vector product transforming a sequence of n complex numbers $\vec{x} = [x_0, \dots, x_{n-1}]^T$ into another sequence $\vec{y} = [y_0, \dots, y_{n-1}]^T$. For $k = 0, \dots, n - 1$,

$$y_k = \sum_{j=0}^{n-1} \omega_n^{kj} x_j, \quad (2.21)$$

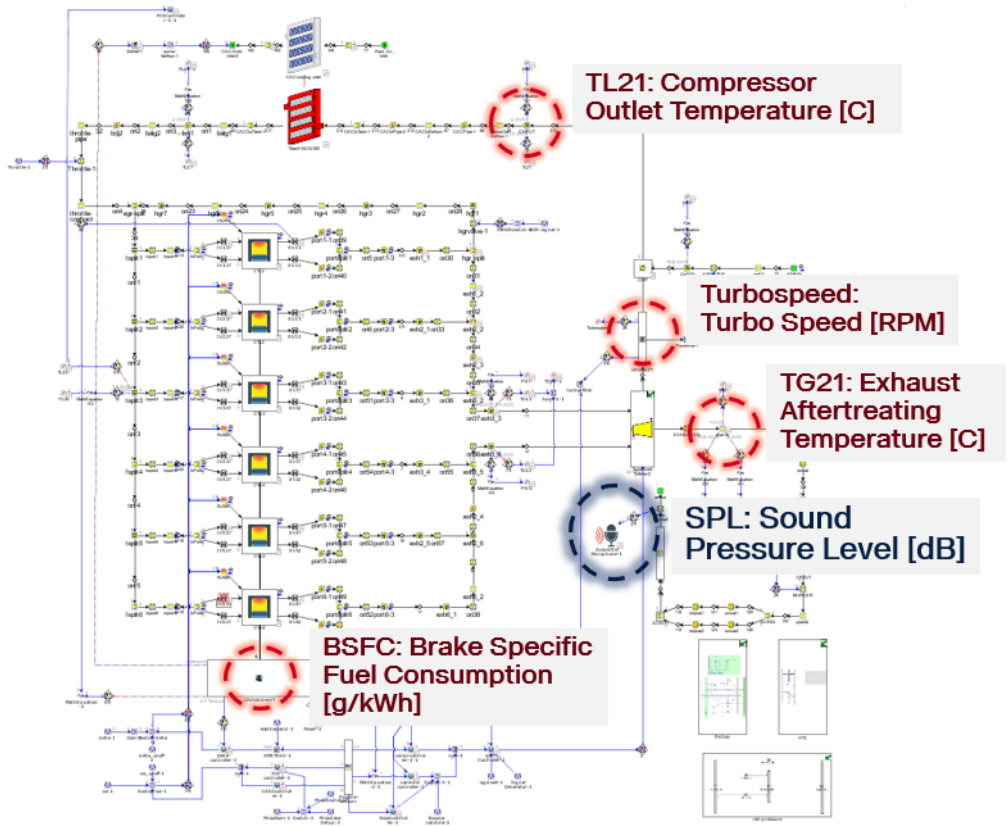


Figure 2.4.1: Illustration of the GT-Power model. Here the virtual microphone is marked in blue, whilst the parts at which constraints are measured are marked in red.

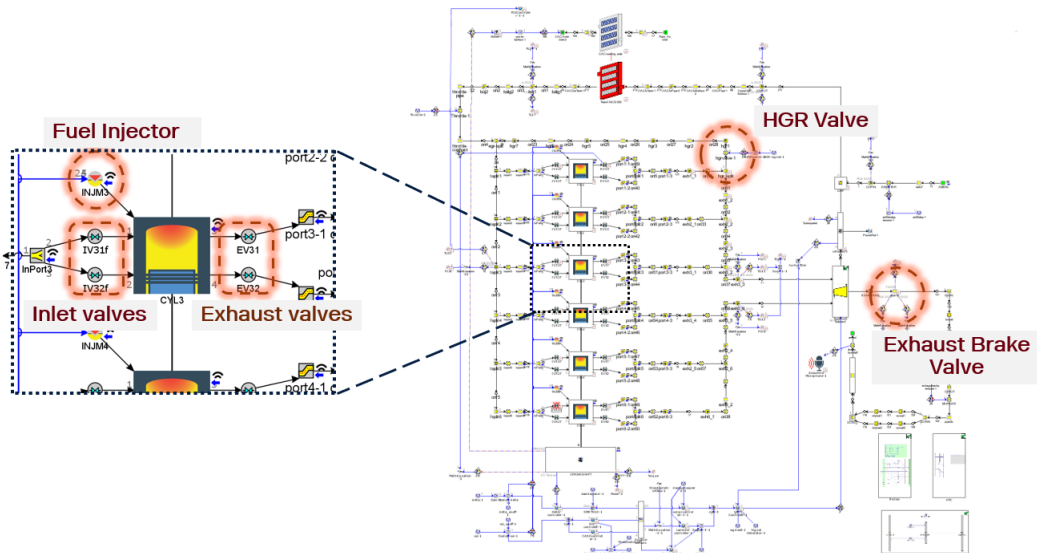


Figure 2.4.2: Illustration of the GT-Power model with the design variables' positions are marked in red.

where

$$\omega_n = \cos\left(\frac{2\pi}{n}\right) - i\sin\left(\frac{2\pi}{n}\right).$$

In matrix vector form, (2.21) is written

$$\vec{y} = F_n \vec{x}, \quad (2.22)$$

where F_n is the n -by- n DFT matrix. Computing the DFT directly has the complexity $\mathcal{O}(n^2)$, but by factorizing the DFT-matrix into a product of sparse factors, the complexity is reduced to $\mathcal{O}(n\log_2 n)$ for the FFT which is very powerful when large data sets are considered. [4]

2.4.2 Optimization in GT-Power

The built-in optimizer in GT-Power, named Design Optimizer, uses a search method or a deterministic algorithm in order to minimize or maximize a given objective function. The optimizer runs iteratively and uses the result from previous steps to determine a new set of independent variables in order to approach the optimal solution [15, Chapter 2]. The setup includes defining one or more objectives, parameters and constraints. Constraints are handled in a way similar to Lagrangian relaxation, penalizing the result (multiplying with very large positive or negative numbers) to lead the optimizer away from factor values violating the constraint. A simulation output can be considered a non restricted constraint in order to get output data of how it is affected by changes of the design variables. [15, Chapter 1]

The design optimizer in GT-Power uses parameters from the case setup as design variables together with lower and upper limits. Each design variable (factor) is designated as *sweep* or *independent*. For a sweep variable, the optimizer will find a single optimal setting for the full range of speed (all cases), whilst an independent variable is itself dependent of the speed (RPM), thus a single optimal setting is considered for each speed. The number of designs, D , to optimize over is

$$D = I \cdot C + S, \quad (2.23)$$

where I is the number of independent factors, C the number of active cases and S the number of sweep factors. The optimizer can handle up to 40 designs simultaneously, but from equation 2.23, it is obvious that the number of designs grows rapidly with the

number of independent variables and active cases.

For a full range of N different speeds, the full range objective is a weighted combination of the objective of speed $n = 1, \dots, N$. For an optimization result, R_n and a weight w_n for speed n , there are three different possibilities for the combined objective to select in GT-Power:

$$f = \frac{\sum_{n=1}^N w_n R_n}{\sum_{n=1}^N w_n}, \quad (2.24)$$

$$f = \min(w_1 R_1, w_2 R_2, \dots, w_N R_N), \quad (2.25)$$

$$f = \max(w_1 R_1, w_2 R_2, \dots, w_N R_N). \quad (2.26)$$

The weights can be distributed individually for each speed considered. [15, Chapter 2.2.4]

Multi-objective Optimization

The multi-objective optimization is approached by the design optimizer in two ways: Pareto or weighted-sum. The weighted-sum approach is best used when all objectives have similar dependency of the design variable, i.e. they increase and decrease simultaneously when the values changes. The combined objective f , takes the sign of response i , S_i , the response weight for response i , $w_{r,i}$ and the normalization term, $R_{norm,i}$ for response i and is computed as

$$f = \sum_i \frac{S_i w_{r,i} R_i}{R_{norm,i}}. \quad (2.27)$$

For the purpose of this study, such a correlation between acoustic output and fuel consumption can not be expected, thus the Pareto approach will be used primarily when multi-objective optimization is considered. The weighted-sum approach is used once in order to compare results and for evaluation.

The Pareto approach creates a Pareto front which illustrates a trade-off between the different objectives considered by plotting the one response over the other. [15, Chapter 1.3]

Algorithms

The design optimizer uses four different algorithms in order to solve the optimization problems, two search algorithms and two deterministic algorithms. A very brief introduction of the four algorithms is presented here. For further details, see [15, Chapter 2.9], [6], [17], and [20].

- **Genetic Algorithm (GA), NSGA-III/Accelerated GA,** Search algorithm:

NSGA-III was developed for many-objective optimization (more than two objectives). It starts with a population and a set of reference points widely spread over a unit hyper-plane with the idea that one population member is expected to be found for every reference point. It yields a Pareto front to show the trade-off for the different objectives. [6]

The Accelerated GA is an extension of the NSGA-III performing better as the number of factors and/or the number of active constraints increases [15, Chapter 2.9.2]. For this project, this algorithm is preferred due to the large number of constraints and factors.

- **Covariance Matrix Adaption Evolution Strategy (CMA-ES),** Search algorithm:

The CMA-ES is a stochastic method for numerical optimization of non-linear, non-convex functions. Evolution strategies are broadly based on the principle of biological evolution where the next generation of candidate solutions are generated by (stochastic) variation of the current parental individuals. Generating new candidate parent solutions for each new generation, the objective is expected to converge towards its optimum. [17]

- **Nelder-Mead Simplex,** Deterministic algorithm:

A numerical method which, at any stage of the algorithm, supervises $n + 1$ points of interest in \mathbb{R}^n , whose convex hull forms a simplex. For each iteration, the vertex with the worst function value is replaced by another point with a better value until it converges at a point where no better function value can be found. [20]

- **Discrete-Grid,** Deterministic Algorithm:

The Discrete-Grid algorithm provides a simple, deterministic approach which repeatedly bisects the search space to select a new search interval in which further

search is performed. The method terminates once the smallest allowed bisection is reached. [15, Chapter 2.9.5]

Each algorithm can either be selected manually or automatically. The design optimizer will choose a search algorithm according to Figure 2.4.3. For the manual selection, Table 2.4.2 presents a summary of properties relevant for the choice of method.

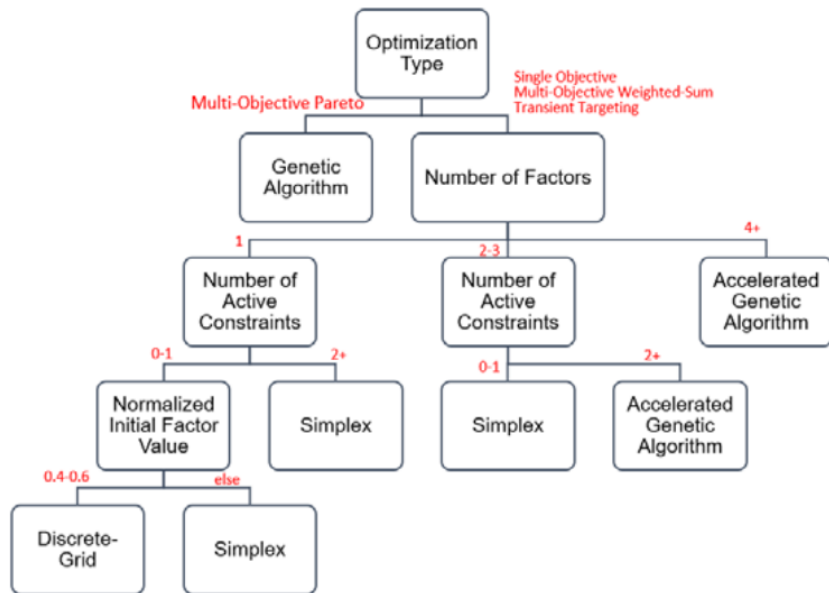


Figure 2.4.3: The selection logic of the automatic selection option in the Design Optimizer of GT-Power [15, pp. 45].

	GA	CMA-ES	Nelder-Mead	Discrete-Grid Simplex
Global/local search	Global	Global	Local	Global
Repeatability	Stochastic	Stochastic	Deterministic	Deterministic
Parallel-Capable	Yes	Yes	No	Yes
Pareto Capable	Yes	No	No	No
Weighted-Sum Capable	Yes	Yes	Yes	Yes
Integers-Only Factors	Yes	Yes	No	No

Table 2.4.2: Specifics of the optimization algorithms in the Design Optimizer of GT-Power [15, pp. 46].

2.4.3 Parallel Simulations, DoEs

GT-Power provides a tool to compare simulation results from different parameter settings for each speed (case) investigated. The parameters investigated are set up as DoEs, where the number of levels as well as the minimum and maximum limits are selected. Each parameter selected will be assigned a number of values corresponding to the number of levels chosen, equally distributed within the set range. As an example: Given a parameter $x \in [x_a, x_b]$. If x is set as a DoE, the lower limit x_a as well as the upper limit x_b are given together with a number of levels, k . For $x_a = 0, x_b = 10, k = 3$, the simulation will run each case for three different x -values: $x_1 = 0, x_2 = 5, x_3 = 10$. Adding more parameters as DoEs, the number of experiments each case increases rapidly as all possible combinations are considered.

Chapter 3

Method

The optimization problem that arises is solved using simulations. In this section, a description of the strategy is presented, followed by details of the setup for the simulations. The section ends with a description of how the analysis is executed.

3.1 Strategy

To attack the complex problem given, an iterative process is executed in order to evaluate and improve the simulation methods along the way. Continuous consultancy with the experienced specialists of their field at Scania is an important part throughout this process.

3.1.1 Baseline Simulation

With a GT-Power model of the CBE1, a baseline simulation is performed. This baseline constitutes a framework for how the optimized model should perform. The acoustic output from this baseline model sets the target of which the optimized model should outperform.

3.1.2 Sub-problems

Despite the non-linearity of the problem, initial runs are performed where individual parameters are varied one by one. This is mainly to document and understand how each parameter affects the acoustic output and to outline the non-linear behaviour as

more parameters are added. Beyond that, specific ranges of interest can be identified for each parameter which will decrease the number of design variables for the full optimization problem.

Simulations are also performed for one or just a few speeds at the time. This is also part of the initial investigation in order to reduce complexity for the full problem. The time complexity is already high for simulations over the full range of speed, investigating all parameters for the full range at once is therefore not a good option.

3.1.3 Optimization and DoEs

The first option to find the optimal model is to use the Design Optimizer provided within GT-Power. This has not been used before at Scania for acoustic problems with this complexity, hence a part of this project is to investigate how it performs for such problems. DoE simulations will thus be run in parallel with the Design Optimizer in order to map its behaviour and evaluate if the results are accurate. Depending on the outcome of the design optimizer simulations, a strategy for the continuation of the project is taken in order to find the optimal design.

The DoE simulations are accurate from that aspect that the different designs are controlled by the user as each value tested is pre-defined. For a parameter simulated as a DoE, an upper and lower limit is given as well as the number of levels studied (e.g. For lash between 0 and 1 mm with three levels, 0 mm 0.5 mm and 1 mm will be simulated). In comparison with the optimizer, which tries to converge at an optimal solution, the DoE will only return the simulated result from the given input, regardless of an objective function. In order to find the optimal value, each simulation must be analyzed individually in order to find a finer set of the parameter setting. As this iterative process precedes, it can in some sense be considered a non-automated optimization algorithm.

3.1.4 Evaluation

The results from the design optimizer as well as for the DoEs are evaluated with respect to their effect on acoustics and their feasibility. This is in order to refine intervals and improve the setup for new simulations. At this step of the process, refined parameter settings are expected to be found. As the single-parameter simulations are

documented one by one, parameters can eventually be added to investigate the non-linear effects.

Here, the iterative process starts as the work progresses repeatedly through Section 3.1.2, 3.1.3 and 3.1.4.

3.2 Setup

All simulations throughout this study are performed for different speeds within the operating speed range 600-2000 RPM and at 100 % load (simulating a heavily loaded truck travelling uphill).

Regarding the constraints, given limits are presented in Table 3.2.1 as well as Figures 3.2.1a and 3.2.1b. The exhaust after treating temperature (TG21) and the BSFC are case dependent thus presented as diagrams with given limit over each speed. All other settings are kept unchanged throughout this project. Specific details about the model and settings are omitted here.

Parameter	Name	Maximum value
Exhaust after treating temperature	TG21	- ° C (case dependent)
Compressor outlet temperature	TL21	38.0880 ° C
Turbo speed	Turbospeed	104000 RPM
BSFC	BSFC	- g/kWh (case dependent)

Table 3.2.1: Limits for control output constituting the feasible region (TL21 is scaled due to confidentiality).

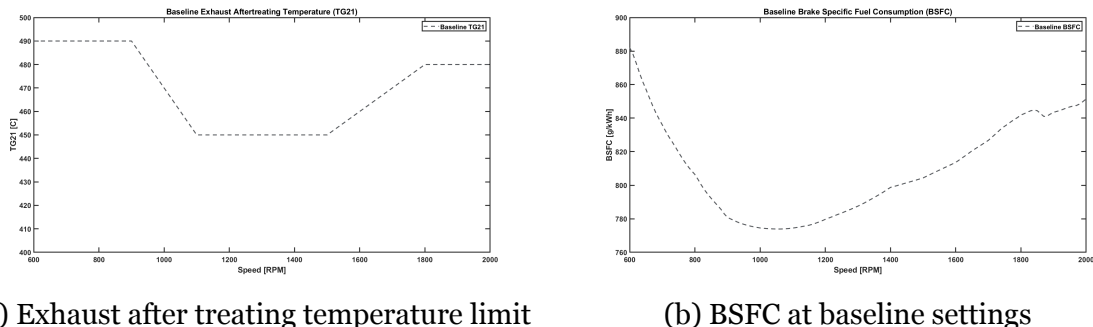


Figure 3.2.1: TG21 limit and baseline BSFC (numbers are scaled).

Baseline settings and given ranges for the design variables are presented in Table 3.2.2. For the baseline, all settings considering the cylinders are set equally for all

Parameter	Name	Range	Baseline
Lash, inlet	Ilash	[0, 1] mm	0.5 mm
Lash, exhaust	Elash	[0, 1] mm	0.1 mm
Fuel injection	Delta	[0, ∞) mg	- mg (case dependent)
HGR valve	HGROnOff	0,1	0, (Closed)
Exhaust brake (diameter)	DPUpperEvap	[0,110] mm	110 mm
Cam timing angle, inlet	Intaketim	[0°, 90°]	0°
Cam timing angle, exhaust	Exhausttim	[-90°, 0°]	0°

Table 3.2.2: Baseline settings and initial ranges for the design variables.

six cylinders. The exact amount of fuel injected is derived by the PID-regulator and omitted here since it is only a relative change which is concerned.

The acoustic output is measured at the outermost orifice of the exhaust system using the GT-power tool 'AcoustExtMicrophone'. It is set up to include flow noise and measures simulated sound generated by the engine and the exhaust system up to 4000 Hz.

3.3 Results and analysis

The results from the simulations are given and visualized in GT-Post, another software within the GT-Suite. For this study, the output data of interest is exported to Matlab and/or Excel for processing and uniform result presentation.

For all simulations performed, (regardless if a basic simulation, DoEs or the design optimizer is used) the output of the objective as well as the constraints are given. The optimizer also provides specific output data and graphs showing how the constraints are affected by the different designs considered as well as detailed data about the settings of each design.

Chapter 4

The Procedure

During this project, simulations are being performed continuously with updated values as the results from previous runs are evaluated. The Design Optimizer as well as the DoEs are used in order to compare and confirm the results of the different approaches. The results are also discussed with the experts of their field around several departments at Scania. Cases yielding ambiguous results using the Design Optimizer are investigated further using DoEs to study the origin.

4.1 Baseline Setup

A baseline simulation is performed with all parameters set as the model is given by the design team. This result is set as a target for the optimization. The baseline model is given for the full operating speed range, initially with step size 100 RPM. In order to follow smaller differences and fluctuations as the final comparison is performed, the settings are interpolated linearly to cover the range with step size 10 RPM. The linear interpolation is chosen by convention. Only the baseline model and the final optimized model(-s) are simulated at this finer speed interval due to the long run time. For the $n = 1, 2, \dots, 15$ steps with step size 100 RPM, the interpolated values are computed for $j = 1, 2, \dots, 100/10$, $i = 1, 2, \dots, 141$ steps with step size 10:

$$u_i = u_n + (j - 1) \frac{u_{n+1} - u_n}{j_{max}} \quad (4.1)$$

The interpolated values are compared with the given baseline with step size 100 RPM. The result from this comparison shows zero difference thus the interpolated values are

confirmed to be accurate.

As already mentioned, the CBE1 has a very high fuel efficiency thus it is not expected to be decreased further within this study. The target for the optimization is therefore to keep it on similar levels or show a possible trade-off on fuel consumption for lower acoustic output.

The fuel injected is controlled by a PID-regulator, presented in Section 2.2.2. This can be turned off to manually control the fuel injection and investigate the acoustic behaviour when the amount of fuel is varied. The amount of fuel injected in the baseline simulation with the PID-regulator switched on is given as input for the simulations where the PID is switched off. A DoE-simulation is run for the PID-regulator being on and off in order to confirm that the output of these runs are equal.

4.1.1 Updated setup

The baseline model does not allow for the parameters to be set individually. A modification of the model is therefore required in order to use individual settings for the fuel injection and the cam timing angle. The remodelling is made in a later stage of the process, hence the first simulations does not cover the fuel injection and the cam timing angle. In the updated setup, the valves and injectors are modified and the PID-regulator is switched off in simulations where the amount of injected fuel is adjusted manually.

The updated setup injects different amount of fuel for all six cylinders which are controlled by six separate gain-components in the GT-Power model. With this gain, the fuel injected is varied $\pm 5\%$ from the fixed value (the value computed using the PID-regulator with baseline settings).

4.2 First Optimization Simulations

When evaluating the applicability of the Design Optimizer to this problem, the results accuracy and validity requires careful consideration. The Design Optimizer runs a number of designs, each with individual settings for the different factors. Besides finding an optimal design, the Design Optimizer also returns detailed data and plots showing how each factor has been varied over the different designs. How the objective(-s) are affected by each design, as well as the feasibility of each design

Parameter	Min	Max	Unit	Type
Lash, inlet	0	1	mm	continuous
Lash, exhaust	0	1	mm	continuous
Exhaust break valve opening	0	1	mm	continuous
HGR-valve	0 (Off)	1 (On)	-	discrete

Table 4.2.1: Parameter settings for first optimization simulation.

simulated is also presented. When finding an optimal design, DoE simulations are performed for the suggested optimal ranges of the factors and the results are compared. For some optimization rounds, the results are obviously inaccurate. For such occurrences, the results are studied in order to find and understand the cause of the erroneous result. Variables concluded to be causing inaccuracy in the simulations are either adjusted in range or excluded from forthcoming simulations.

To focus on evaluating the Design Optimizer itself rather than to reach an optimal design at this stage, only one speed (1500 RPM) is considered. The three different approaches, multi-objective Pareto, multi-objective weighted sum and single-objective, are used on similar cases in order to see if and how the result from the different approaches alter. The best approach according to these first runs is thereafter used on other speeds to eventually cover the full operating speed range. Due to the high time complexity of the optimization rounds, four speeds (600 RPM, 1100 RPM, 1500 RPM and 2000 RPM) are considered enough to evaluate if the Design Optimizer suggests equal optimal designs at different speeds.

First, a multi-objective optimization is performed where the SPL with flow noise included is set as objective together with the fuel consumption, BSFC. The factors are the lash (inlet and exhaust), the exhaust brake valve and the HGR-valve. Constraints are set as given in Section 3.2 for the compressor outlet temperature, the exhaust after treating temperature and the turbo speed. The Design Optimizer chooses algorithm according to 2.4.3. Regardless which optimization type is chosen (single objective, multi-objective Pareto, multi-objective weighted sum) within this project, the accelerated GA is always used. No other algorithms are investigated for this problem since no better result is expected due to the number of parameters and constraints. The specified parameters and their intervals for the first simulations are presented in Table 4.2.1.

From these results, parameters for further simulations are excluded or adjusted in

range as conclusions about their effect on the acoustic output can be drawn from the optimization results. Hereafter, a weighted sum optimization is performed at 1500 RPM with the exhaust brake parameter excluded. Next, single optimization is chosen, again at 1500 RPM and with the BSFC set as an unconstrained constraint to be well monitored. From evaluating the results, the single optimization is selected for further optimization rounds within the project. Additional single-optimization rounds are simulated at 600, 1100 and 2000 RPM in order to consolidate the results for the lash and the HGR-valve settings over different speeds. DoEs are then performed in order to confirm the results of how the acoustic output is affected by the parameter settings.

4.2.1 Including all parameters

As the modification of the model is implemented and the first optimization rounds are complete, one optimization round is performed including all parameters in order to really examine the capability of the Design Optimizer. The complete optimization problem is given as input, 16 factors in total. The factors' ranges are narrowed to some extent according to the results of the first simulations. Due to the time complexity, this optimization only covers the main target speeds 1400, 1500, 1600 and 1700 RPM. Specifics of the full optimization setup is given in Table 4.2.2. For this optimization round, the minimum value over all operating speeds is targeted (i.e. according to equation (2.25)).

From the result of this optimization (presented and discussed in chapter 5 and 6) the number of parameters is decreased. A second large optimization is performed with the cam timing angle excluded, decreasing the number of parameters to 10. Even though it was concluded that the exhaust brake valve should be completely open for the engine to operate properly under the conditions for the pass-by-test, the exhaust brake valve is included in this simulation. This is mainly out of two reasons: Firstly in order to evaluate the capacity of the Design Optimizer, and secondly in order to monitor the parameters' non-linear behaviour. Thenceforth a third optimization round is performed where also the exhaust brake valve opening is excluded in order to find a viable solution corresponding to how the engine is operating under the pass-by test conditions. The results are compared with what is known from previous simulations.

Objective Function	AcousticExtMicrophone: SPL plus Flow		[dB]
Constraints	TL21: Compressor outlet temperature	38.0880	[°C]
	TG21: Exhaust After treating temperature	Case dependent	[°C]
	Turbo Speed	104000	[RPM]
Design Variables	Inlet valve lash	[0.35, 1]	[mm]
	Exhaust valve lash	[0.35, 1]	[mm]
	Exhaust brake valve opening	[35, 110]	[mm]
	HGR valve	1, 0	[-]
	Gain of fuel (%) on injector 1	[95, 105]	[-]
	Gain of fuel (%) on injector 2	[95, 105]	[-]
	:	:	
	Gain of fuel (%) on injector 6	[95, 105]	[-]
	Intake cam timing angle cylinder 1 & 6	[0, 90]	[°]
	Intake cam timing angle cylinder 2 & 5	[0, 90]	[°]
	Intake cam timing angle cylinder 3 & 4	[0, 90]	[°]
	Exhaust cam timing angle cylinder 1 & 6	[-90, 0]	[°]
	Exhaust cam timing angle cylinder 2 & 5	[-90, 0]	[°]
	Exhaust cam timing angle cylinder 3 & 4	[-90, 0]	[°]

Table 4.2.2: Setup for the full optimization problem. (TL21 and TG21 constraints values are scaled).

4.2.2 Design of Experiments

DoEs are performed for the lash, the HGR-valve, the cam timing angles and the fuel injection respectively. Most DoEs are simulated at 600, 1100, 1500 and 2000 RPM to investigate if the trend is consistent over the full range of speed but yet keep the number of simulations down. For the fuel injection DoEs, the amount injected is varied $\pm 5\%$ only on the first three cylinders in order to keep the run-time down.

4.3 Results Analysis

A first, brief results analysis of the Design Optimizer output can in most cases be performed directly using the GT-Post software which displays several plots showing the progression of the optimization. A deeper analysis is performed using Matlab and/or Excel. The analysis is performed by filtering and plotting all or selected sequences of the data. In Excel, conditional formatting is used to generate heat maps over the result. The data from the different optimization rounds is also compared in order to find similarities and deviations for the different setups.

The DoE simulations does not generate plots as detailed as the design optimizer. Thus

the data is in most cases collected and analyzed directly using Excel and/or Matlab. For the DoE results, plotting the numbers in Matlab together with baseline results as well as the constraints constitutes the majority of the work.

From the analysis, areas of specific interest are identified which can be investigated further. Mainly in order to finer the intervals for the parameters' ranges, but also to find areas of interests suggested to be investigated further in future work.

As the knowledge about the acoustic effects from the parameter settings increases and as the model is refined throughout the process, new findings are discovered which sometimes contradicts the initial strategy. In these cases, the expected outcome of such discoveries are discussed in Section 5. If possible, simulations are re-made in order to determine the effect from such a different setting. In other cases, further investigation is instead left for future work.

4.4 The Optimal Solution

As the analysis is executed, a final, optimal design takes shape. The best design is simulated over the finer speed interval, 600-2000 RPM with step size 10 and compared with the baseline settings. Here, a number of optimal solutions are presented as the circumstances for how the settings can be made varies, but also since the simulation settings are considered contradicting to how the actual engine operates. Different designs are presented in order to better understand what affects the acoustic output the most and how to execute future research on the area.

Chapter 5

Results

Here, the results from the simulations are presented, in most cases together with a short comment or conclusions regarding parts of the work. Final conclusions, further discussions and suggestions on future work based on the results shown here are left for the next section, Section 6.

Due to confidentiality, the results considering BSFC and the constraining temperatures (TG21, TL21) are scaled.

5.1 Baseline

Results of the baseline simulation considering the acoustic output, the BSFC and its feasibility are shown in Figures 5.1.1 and 5.1.2. The result of this simulation is set as target for the following simulations and optimizations. Regarding the feasibility, note the violation on the turbo speed constraint at about 1700 RPM. (A zoomed-in plot of the trampling is given in Figure 5.1.3.) Engine performance varies at different altitudes as the density of the air changes and a suggestion to the trampling of the constraint is that the altitude settings differs for the constraint and for the settings used here. Given limits does thus not fully correspond to the altitude at which the simulations are performed (0 m above sea level) which probably causes the violation. Small violations can in general be ignored, as for the case here. Nevertheless, considering the optimization problem, possible effects of inexactly stated constraints is further discussed in Section 6.1.1.

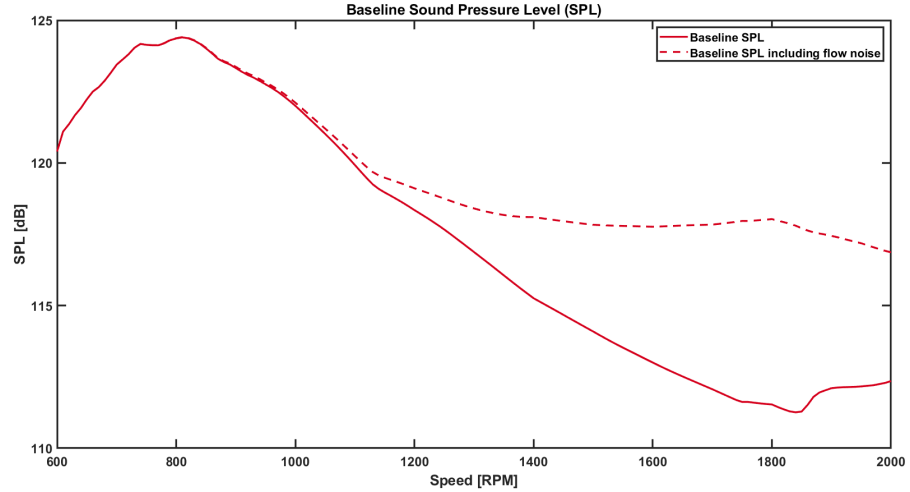


Figure 5.1.1: Sound pressure level with flow noise included and excluded respectively at baseline settings.

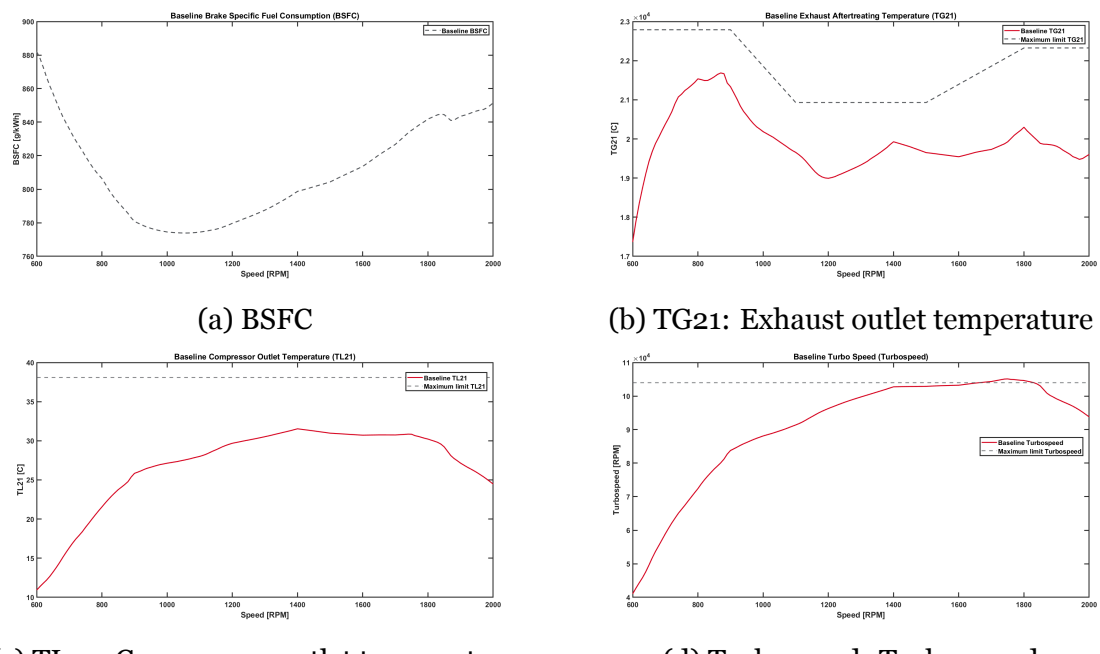


Figure 5.1.2: Output results at baseline settings together with given limits for maximum values.

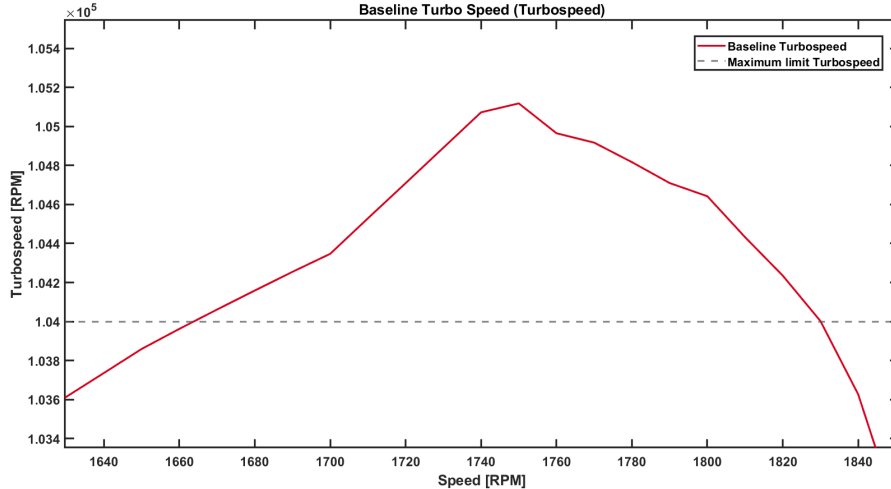


Figure 5.1.3: A zoomed in plot of Figure 5.1.2d showing the trampling of the turbo speed limit at baseline settings. The infringement is ongoing between 1670 and 1830 RPM and is at most 1118 RPM over the limit (104000 RPM, i.e. 1.07 % above the limit).

5.2 Optimization

The results from the different optimization rounds are shown here. In most cases, the objective function(-s), SPL including flow noise and the BSFC are presented. Beyond that, plots showing the convergence of the design variables are presented in cases where they are considered to add value to the analysis. Further results of e.g. different speeds that may be relevant to the interested reader can be found in appendix A.

5.2.1 First Optimization:

Valve Lash, HGR-valve, Exhaust Brake Valve

As stated in Section 3.1, smaller sub-problems are considered initially. Since the model requires re-modification to handle individual settings for the cam timing angle and fuel injection, a natural selection of components within the first optimization are valve lash, HGR-valve and exhaust brake valve.

Multi Pareto Optimization

The first optimization is a multi-objective Pareto optimization considering lash (inlet and exhaust), HGR-valve and exhaust brake valve. The result is shown by a Pareto front where the two objectives (the sound pressure level and the brake specific fuel

consumption) are plotted together with the baseline levels, see Figure 5.2.1. The extreme values of the BSFC (compare with baseline, Figure 5.1.2a) shows obvious inaccuracy of the result. Figure 5.2.2 displays the two objectives separately as functions of the exhaust brake valve opening. From Figure 5.2.2a it is without difficulty concluded that the inaccurate result appear as the valve opening is below approximately 55 mm. The acoustic behaviour from this simulation as a function of the exhaust brake valve opening is seen in Figure 5.2.2b.

Under the conditions of a pass-by noise test, the engine will not operate with the exhaust brake valve closed to any degree, thus the result from this optimization is observed, but further simulations are essentially performed with the exhaust brake valve completely open. Results regarding the design variables and their suggested optimal values are considered inaccurate within this optimization thus new simulations are performed where the exhaust brake valve is no longer considered. For additional investigations including the exhaust brake valve (see Section 5.2.2) the smallest value allowed is set to 55 mm in order to simulate accurately.

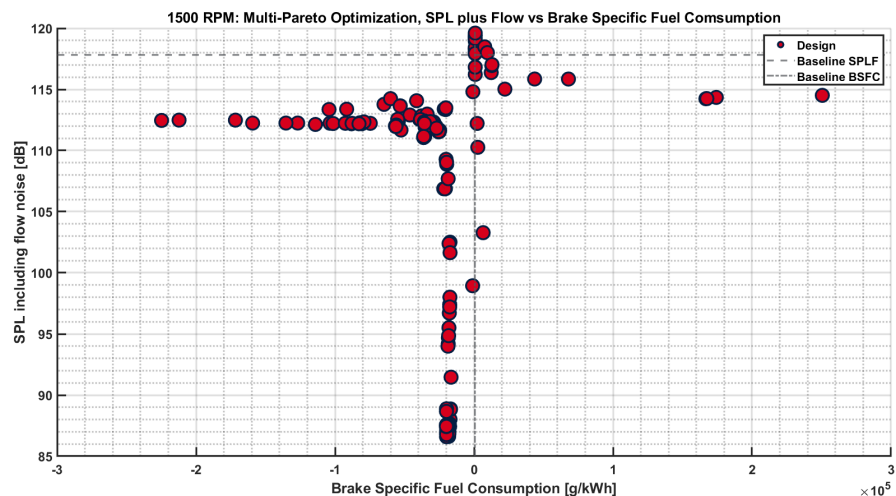


Figure 5.2.1: Pareto front of the first multi-objective optimization showing the BSFC and the SPL including flow noise for each design generated.

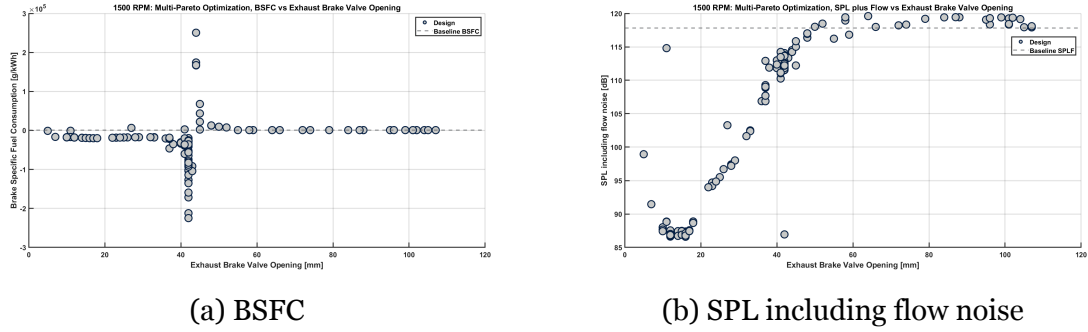


Figure 5.2.2: Brake specific fuel consumption and sound pressure level including flow noise together with baseline levels as functions of the exhaust brake valve opening.

Single Optimization

The next optimization approach is the Single-objective optimization, now with the exhaust brake valve excluded. The BSFC is now monitored as a non-restricted constraint. The inlet and exhaust valve lash and the HGR-valve are set as design variables at 600, 1100, 1500 and 2000 RPM. Figure 5.2.3 shows the the SPL including flow noise as it evolves towards its optimum value for each iteration and new design considered. In Figure 5.2.4, the design variables' value for each design is seen, showing a clear convergence towards their optimal values. Looking at the fuel consumption, Figure 5.2.5 shows the BSFC, where a desired decrease in fuel consumption is indicated. The behaviour is similar for both inlet and exhaust valve lash at all speeds considered. Results and plots for the other speeds (600, 1100, 2000 RPM) can be found in appendix A. Regarding HGR-valve opening, the optimal design suggests the valve to be turned Off at 1100, 1500 and 2000 RPM, whilst it is suggested to be turned On at the lower speed, 600 RPM.

In order to confirm the results and to investigate the different optimal suggestions on HGR-valve at the lower speed further, DoEs are simulated for the lash and the HGR-valve respectively. Other settings are kept unchanged (from baseline levels) as these parameters are varied. For the HGR-valve, the full speed range is simulated for the two options available. Results are shown in Figure 5.2.6. It is clear that the suggested optimal settings corresponds well with the DoE results and it can be seen that the interchange from lower noise with the HGR-valve On to HGR-valve Off is somewhere around 1100 RPM.

Considering the lash, a DoE is simulated varying the inlet and exhaust valve lash between 0 and 0.5 mm simultaneously (larger lash is not considered interesting for

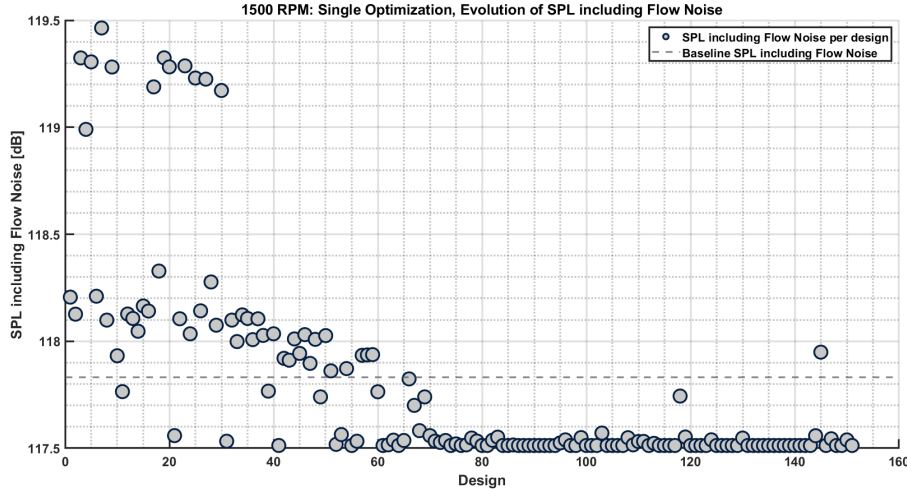


Figure 5.2.3: Sound pressure level including flow noise at 1500 RPM. Evolution over each design using the Design Optimizer.

the purpose to verify the optimization result). The simulation is set with 5 levels, which gives measuring points at 0.0, 0.125, 0.25, 0.375, and 0.5 mm. This yields 25 designs for each speed simulated. Here, the result for 1500 RPM is shown in Figure 5.2.7. The first design corresponds to 0 mm lash on both inlet and exhaust valve. As seen, the acoustic output is at its lowest value at this first design, which verifies that the Design Optimizer has suggested parameter settings corresponding to the lowest acoustic output. The suggested optimum setting output is shown by the dashed lines for the acoustic output with and without flow noise included. For results considering the other speeds (600, 1100, 2000 RPM) the same conclusion can be drawn. For details, the reader is again referred to appendix A. From the results of the DoEs, the settings suggested by the Design Optimizer can be considered accurate.

A summary of the optimal design settings suggested is presented in Table 5.2.1.

Parameter	Suggested Optimal Setting
Inlet valve lash	0 mm (all speeds considered)
Exhaust valve lash	0 mm (all speeds considered)
HGR-valve	On, speeds < 1100 RPM Off, speeds \geq 1100 RPM

Table 5.2.1: Suggested optimal settings of the design variables considered in the single optimization using the Design Optimizer. The speed for the interchange in HGR-valve setting is taken from the DoE results.

CHAPTER 5. RESULTS

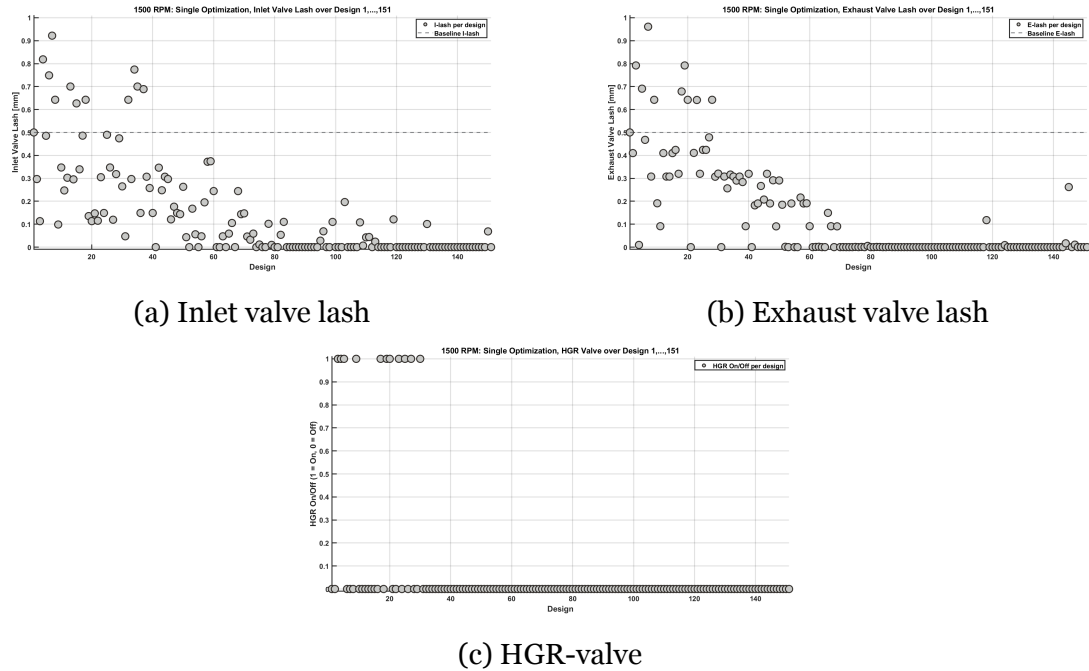


Figure 5.2.4: Convergence of the design variables using the Design Optimizer for single optimization at 1500 RPM, minimizing the sound pressure level including flow noise.

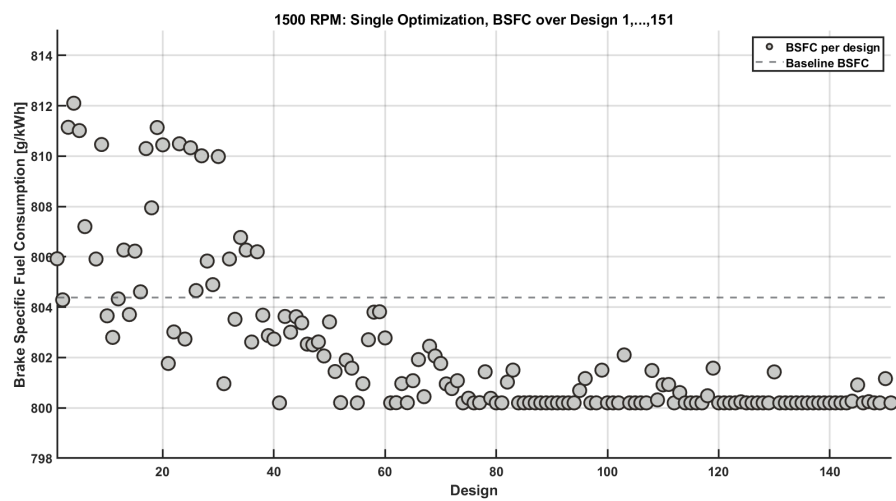


Figure 5.2.5: Brake specific fuel consumption per design considered.

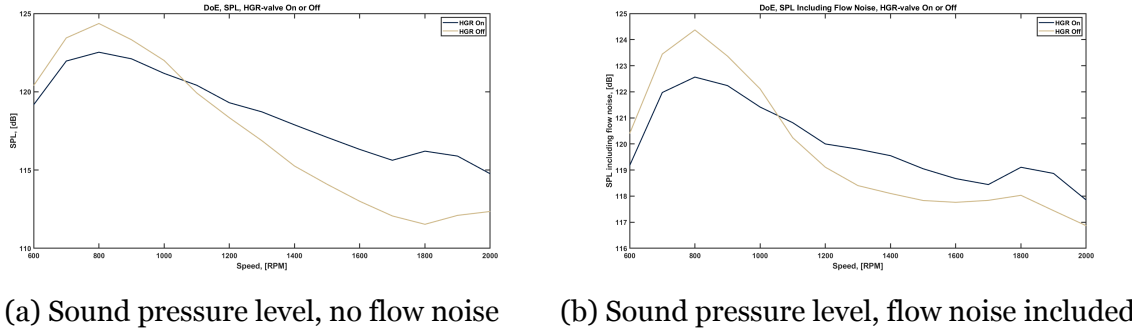


Figure 5.2.6: DoEs for the HGR valve being switched on and off. The two plots shows the acoustic output without and with flow noise included respectively.

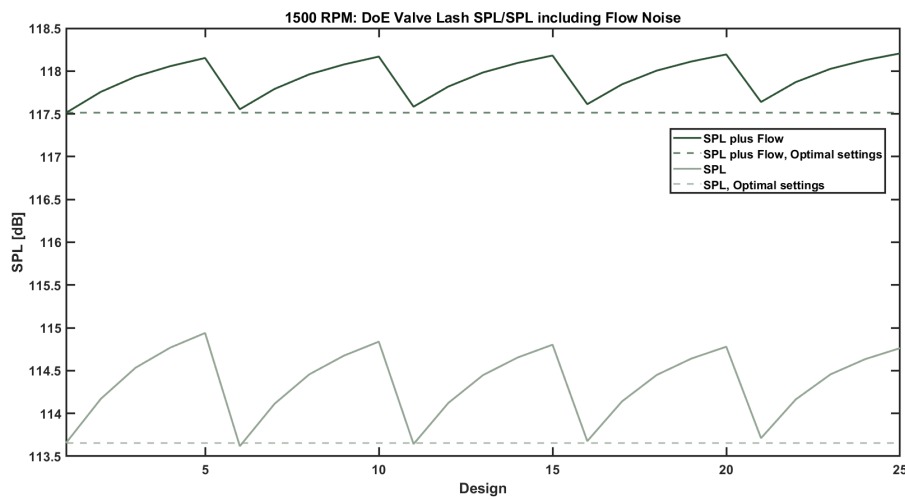


Figure 5.2.7: Acoustic output with and without flow noise included from a DoE simulation at 1500 RPM where inlet and exhaust valve lash are varied. The first design (Design 1) corresponds to 0 mm lash on both inlet and exhaust, thereafter the lash on either one or both valves (inlet and exhaust) are increased until the last design (Design 25) is simulated with 0.5 mm on both valves (inlet and exhaust).

Multi-objective Weighted Sum

One optimization with the multi-objective weighted sum approach is performed at 1500 RPM for the same variables as for the single optimization above (exhaust lash, inlet lash, HGR-valve). The use of different approaches is mainly to compare the results why this one optimization is considered enough. The two objectives are weighted equally. The suggested optimal design settings are equal to the single-objective optimization result (Table 5.2.2). Despite the fact that the approach is not expected to be most favorable for the two objectives here, the optimization shows satisfactory results in line with the single optimization results. A further discussion on this topic is found in Section 6.1.1. Plots from the optimization using the weighted sum approach can be found in appendix A.

It is concluded that all three approaches shows the same accurate result. For simplicity, the single-objective approach will be used henceforth.

Parameter	Suggested Optimal Setting
Inlet valve lash	0 mm
Exhaust valve lash	0 mm
HGR-valve	Off

Table 5.2.2: Suggested optimal settings with the weighted sum approach at 1500 RPM.

Optimal Solution from Initial Optimization

From the initial optimizations performed, it is clear that the acoustic output decreases with smaller lash, both on the inlet and the exhaust side and regardless the HGR-valve setting. The optimal solution suggests 0 mm valve lash, but in order to allow for thermal expansion without causing ware on the mechanical parts, a minimum level for the valve lash on the cold engine is within this project set to 0.35 mm. This limit is used as a lowest value for further optimizations and simulations performed. Note that the baseline settings has the exhaust valve lash at 0.1 mm, i.e. below the smallest limit given. This causes the optimal design with smallest lash allowed, 0.35 mm, to be higher in acoustic output than the baseline model, as seen in Figure 5.2.8 where the baseline and the suggested optimal designs are compared.

Consulting the engine department at Scania, a possible reason to why the baseline

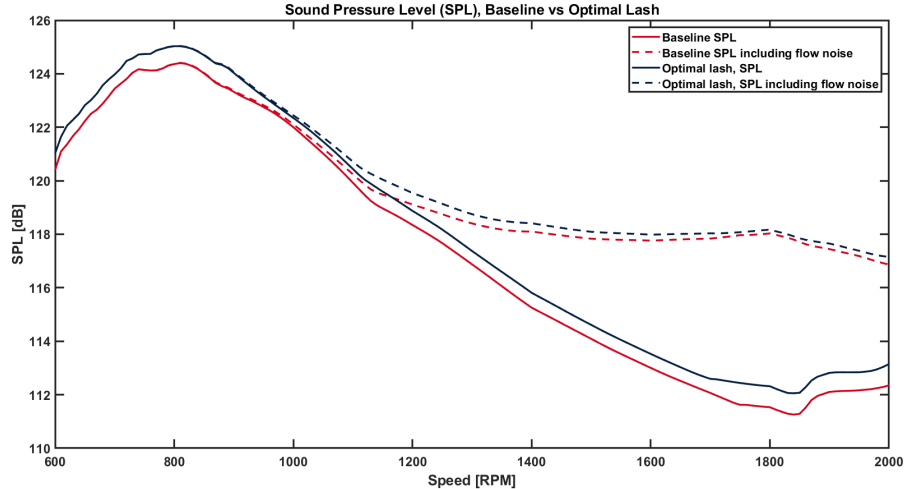


Figure 5.2.8: The design with suggested optimal lash (blue) compared to the baseline setting (red). Note that the simulation is performed with the finer speed interval (step size 10 RPM) hence the less accurate shift for the HGR setting's interchange.

exhaust valve lash can be set to 0.1 mm, is that the cam lifting curve in this simulation model does not take any kinematic effects into consideration and thus yielding an actual lash greater than the value specified in the model. A new cam lifting curve for the valves is provided which is expected to better simulate the actual lift. Since the baseline model provided is the one primarily investigated within this study, the new curve is used as a complement and for further investigation in later stages of the process. The results are shown in Section 5.3 and a further discussion is provided in Section 6.1.2.

Studying the BSFC output using the DoE simulation results, the fuel consumption appears to decrease together with the noise levels as the lash goes smaller (Figure 5.2.9). Considering the HGR-valve, fuel consumption goes up at all speeds as the HGR-valve is on (Figure 5.2.10).

The results presented above are further discussed in Section 6. An extended analysis is also provided there as more simulations are performed and additional parameters are included.

5.2.2 The Complete Optimization Problem

For the full optimization problem, including all 16 parameters as design variables, results are shown in Figure 5.2.11. It is again obvious that the result is inaccurate in view of the extreme values that the BSFC assumes (Figure 5.2.11b), but also due to the

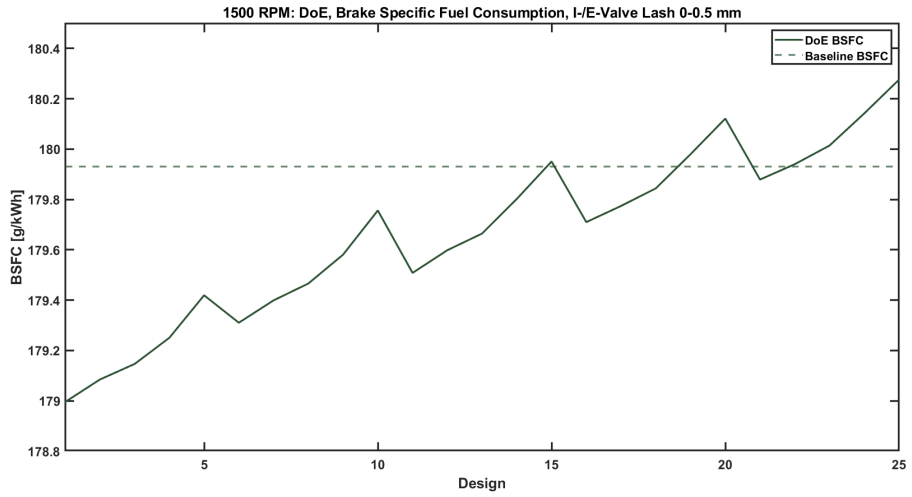


Figure 5.2.9: Brake specific fuel consumption for DoE simulation for the inlet and exhaust valve lash. The first design (Design 1) corresponds to 0 mm lash on both inlet and exhaust, thereafter the lash on either one or both valves (inlet and exhaust) are increased until the last design (Design 25) is simulated with 0.5 mm on both valves (inlet and exhaust).

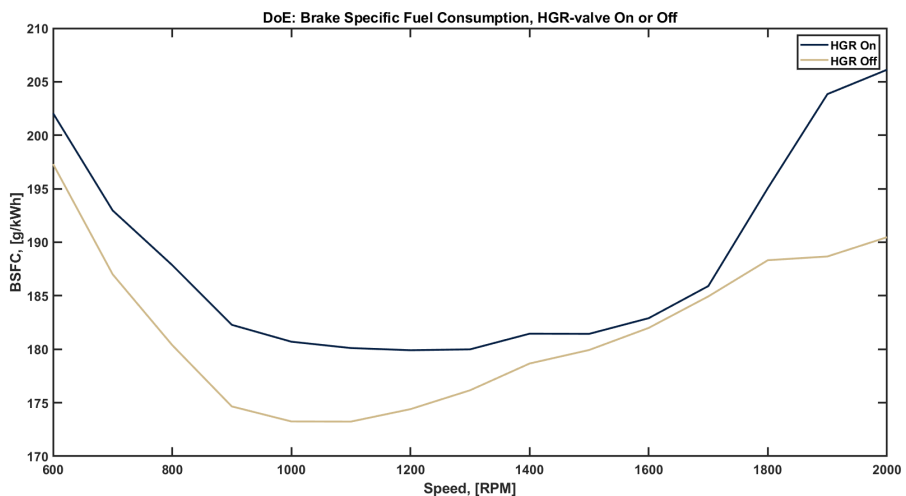
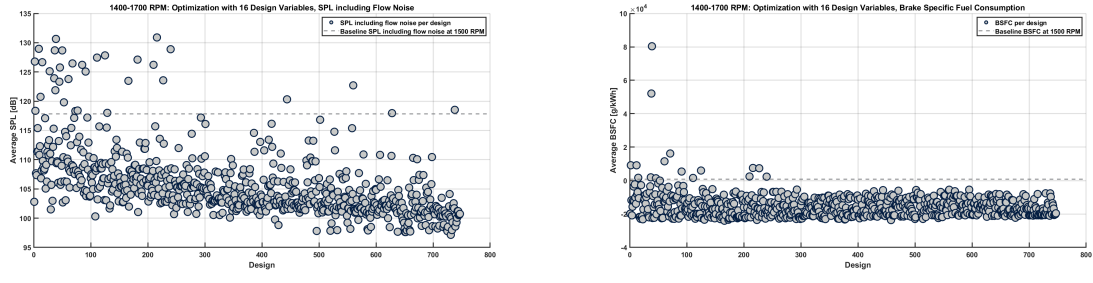


Figure 5.2.10: Brake specific fuel consumption for DoE simulation for the HGR-valve turned On and Off.



(a) Sound pressure level including flow noise

(b) Brake specific fuel consumption

Figure 5.2.11: Average acoustic output and fuel consumption over the speeds simulated (1400-1700 RPM) for the complete optimization problem using the Design Optimizer.

unreasonably low acoustic output level (Figure 5.2.11a) with a minimum 96.42 dB at 1700 RPM and the lowest average over 1400-1700 RPM at 97.15 dB, about 20 dB drop from the baseline level.

Looking at the result from this optimization directly in GT-post¹, it is clear that none of the variables converges to a suggested optimal value but are fluctuating over the full ranges even for the final designs simulated. The result is not considered accurate under any circumstances.

By reason of the extreme values the cam timing angle varies over with given settings, it is primarily assumed to have caused the inaccurate results. In order to confirm this assumption, a simulation with the cam timing angle set as DoEs is performed. The result is shown in Figure 5.2.12.

Another DoE is simulated when varying the fuel injection to eliminate the possibility that this parameter also causes the inaccurate results, see Figure 5.2.13c. The DoE results for the other speeds will be discussed in Section 6.2.1. It is concluded that it is indeed the cam timing angle which causes the erroneous results. Possible reasons to the inaccuracy and suggested solutions are further discussed in Section 6. Due to the complex simulation model, the cam timing angle is decided to be ruled out from further investigation.

¹Not shown here due to the overall inaccurate result

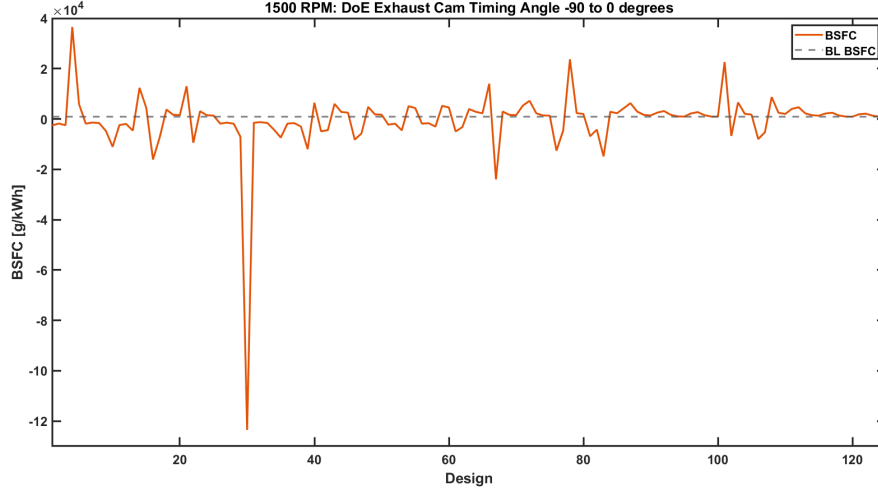


Figure 5.2.12: Simulation of the brake specific fuel consumption with the exhaust cam timing angle as DoE varied between -90 to 0 degrees at 1500 RPM. Cylinder 1, 2, and 3 are varied in order to keep the run time down. Design 1 corresponds to -90 degrees on all three cylinders whilst Design 125 corresponds to 0 degrees on all three cylinders (as for the baseline settings).

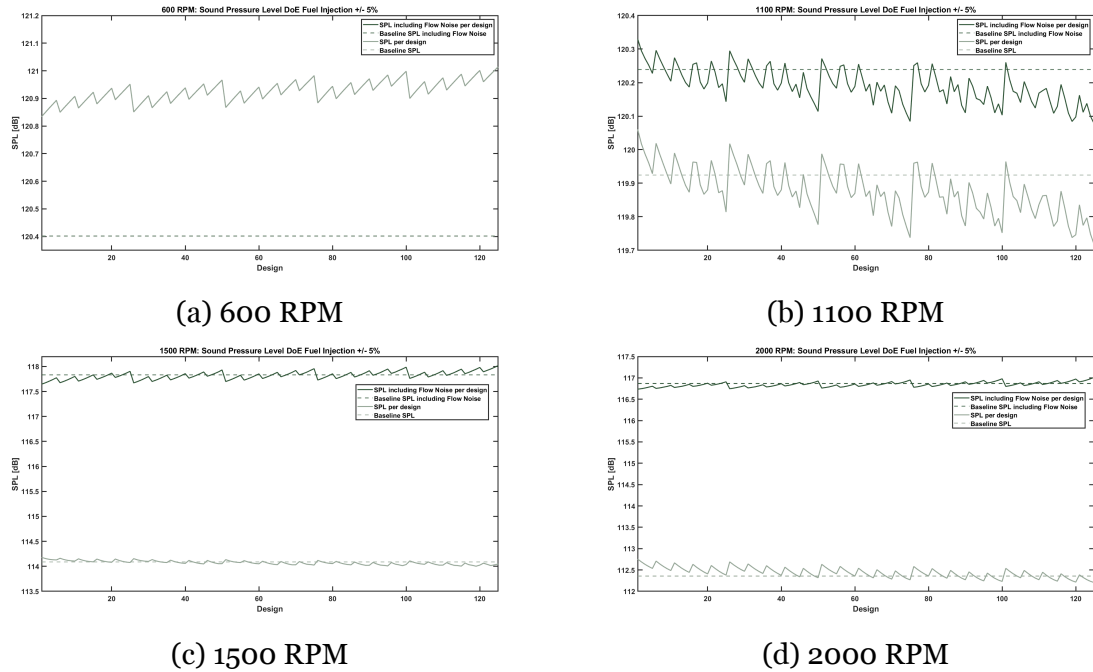
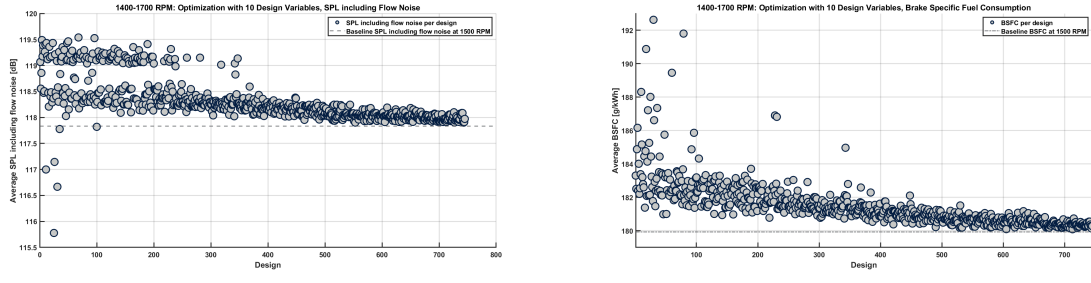


Figure 5.2.13: DoE simulation for the fuel injection on cylinder 1, 2, and 3 varied $\pm 5\%$ for four speeds. Design 1 corresponds to -5 % gain on cylinder 1, 2, and 3, whereas Design 125 is simulated with +5 % gain on cylinder 1, 2, and 3.

A Scaled Down Version

Excluding the cam timing angle, the optimization problem contains ten design variables instead. A result with reasonable values in acoustic output and fuel



(a) Sound pressure level including flow noise

(b) Brake specific fuel consumption

Figure 5.2.14: Sound pressure level and brake specific fuel consumption over 751 designs considering fuel injection, lash, HGR-valve and exhaust brake valve. Evolution performed by the Design Optimizer towards settings to minimize acoustic output.

Parameter	Suggested Optimal Setting
Inlet lash	0.68 mm
Exhaust lash	0.36 mm
HGR-valve	Off
Exhaust brake valve	88 mm
Gain, fuel injection _{Cylinder 1}	102.2
Gain, fuel injection _{Cylinder 2}	95.2
Gain, fuel injection _{Cylinder 3}	96.5
Gain, fuel injection _{Cylinder 4}	96.0
Gain, fuel injection _{Cylinder 5}	95.1
Gain, fuel injection _{Cylinder 6}	95.3

Table 5.2.3: Suggested optimal settings for the complete problem (10 variables) at 1400-1700 RPM.

consumption is provided for this simulation as shown in Figure 5.2.14. Note that also the unfeasible solutions are included but not marked here, thus the points with very low acoustic output amongst the first designs in Figure 5.2.14a. An interesting observation is the gap in SPL output amongst the first 200 designs, which can be derived to when the HGR-valve is switched On and Off.

The suggested optimal design from this optimization is presented in Table 5.2.3. The results contradicts the results from previous simulations regarding valve lash and exhaust brake valve settings. Investigating the convergence of the design variables and comparing with previous results, it is assumed that the problem is still too complicated to be handled by the Design Optimizer properly. This could perhaps be improved by adjusting the settings of the Design Optimizer (as discussed in Section 6.1.1).

A third optimization is performed where also the exhaust brake valve is excluded in order to reduce the complexity further (the choice of parameter to exclude is due to

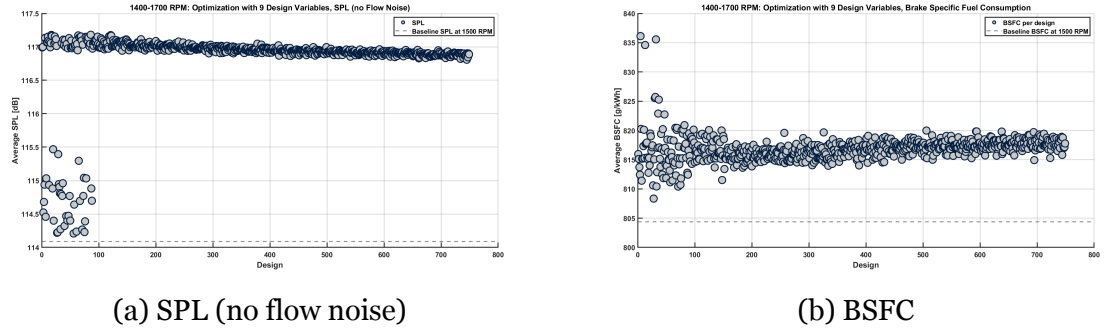


Figure 5.2.15: Sound pressure level and brake specific fuel consumption over 751 designs considering fuel injection, lash and HGR-valve.

the conclusions from the first optimization, Section 5.2.1). Result plots are shown in Figure 5.2.15 and the suggested optimal settings are presented in Table 5.2.4. Note that this optimization has the objective function Sound Pressure Level without flow noise in opposite to the other optimizations performed. This is not considered to affect the result, but mentioned to be reminded when comparing values. Again, the unfeasible solutions are not marked in the figures. The suggested optimal design is contradicting the previous optimization results considering the HGR-valve. This is because all simulations with the HGR-valve Off are considered infeasible². This is further addressed in Section 6.1.2, where the limits for the constraints are discussed as a possible cause. The results from the two large, accurate optimization simulations indicates that the amount of fuel injected has relatively low impact on the noise levels at the prioritized speed (1400-1700 RPM). This is also in alignment with the DoEs simulated for the fuel injection at the speed in question, as shown in Figure 5.2.13. Due to this, and a possible effect of uneven power output when varying the amount of fuel in the different cylinders, the fuel injection is less prioritized for further investigation.

5.3 Adjustments in the Model

As the baseline setting is given with an exhaust valve lash below given minimum limit, a new cam lift curve is provided in order to investigate this further (as mentioned in Section 5.2.1). Figure 5.3.1 shows the two cam lift curves for the inlet and exhaust valves respectively. The new lift curves are suggested to better simulate the actual lift, where the kinematic effects of the lift is included. For the inlet valve lash, the baseline lifting

²Which can be seen by studying the optimization progress in GT-post.

Parameter	Suggested Optimal Setting
Inlet lash	0.39 mm
Exhaust lash	0.43 mm
HGR-valve	On
Gain, fuel injection _{Cylinder 1}	99.1
Gain, fuel injection _{Cylinder 2}	103.7
Gain, fuel injection _{Cylinder 3}	103.1
Gain, fuel injection _{Cylinder 4}	97.4
Gain, fuel injection _{Cylinder 5}	99.0
Gain, fuel injection _{Cylinder 6}	100.3

Table 5.2.4: Suggested optimal settings for the viable problem (9 variables: valve lash, HGR-valve and fuel injection) at 1400-1700 RPM.

curve is given with large steps between the angles, causing the staircase function as the full range (0° to 360°) is covered (Figure 5.3.1a). The accuracy of the actual effect on acoustic output due to changes on the inlet valve lash is thus expected to be improved using this new curve. For the exhaust side in, Figure 5.3.1c shows that the new lift curve is higher than the one for the baseline settings over the full range. The difference, ($C_{new} - C_{old}$) is shown on the right hand side of the figure. The positive difference on the exhaust lift curves can indicate that the actual lash using the baseline lifting curve is in fact greater than the value specified in the simulation settings. Therefore, the minimum limit given (0.35 mm) may already be satisfied at the baseline setting at 0.1 mm. The new curves are expected to better simulate the actual lift and thus yield a more substantial result considering the lash.

The new lift curve shows different dependency regarding the HGR-valve why curves are shown with bot HGR-valve On and Off respectively. Figure 5.3.2 shows the SPL with and without flow noise included for the baseline together with a simulation using the new cam lifting angle and optimal lash (0.35 mm) and HGR-valve On and Off respectively. Since the results shows lower acoustic output using the new curve, and as it is concluded that smaller lash decreases the acoustic output using the baseline curve, the actual exhaust valve lash on the baseline model is most probably higher than 0.1 mm.

Regarding the BSFC for the new cam lifting curve, results are shown in Figure 5.3.3. It is still obvious that the HGR-valve increases the fuel consumption as it is switched On. The very high increase in fuel consumption at the higher speeds requires further investigation.

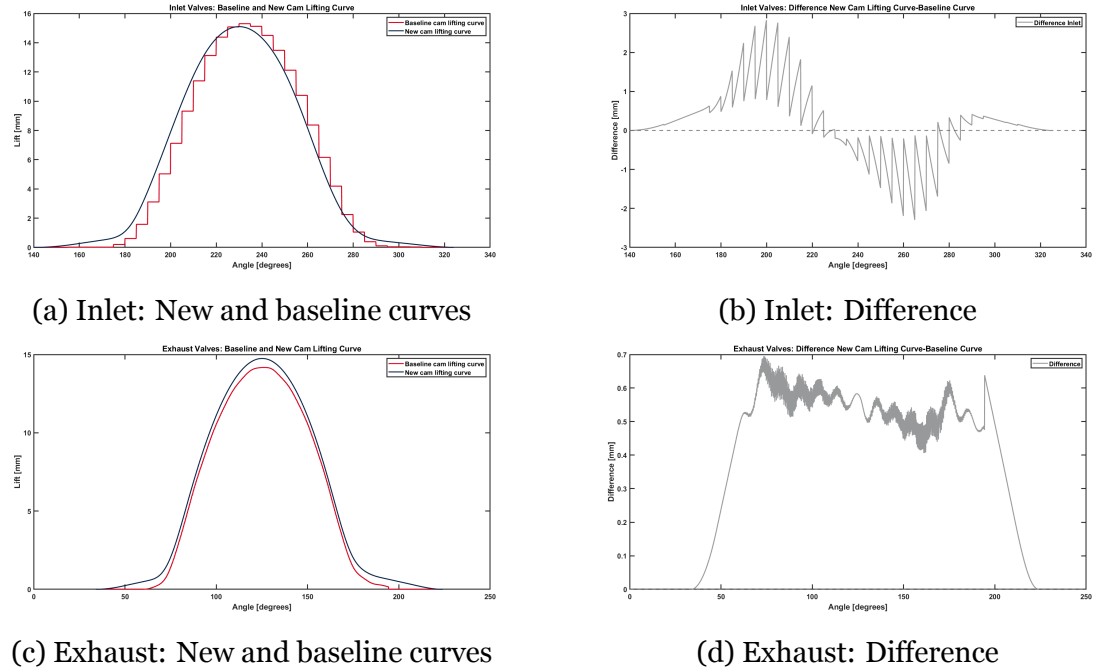
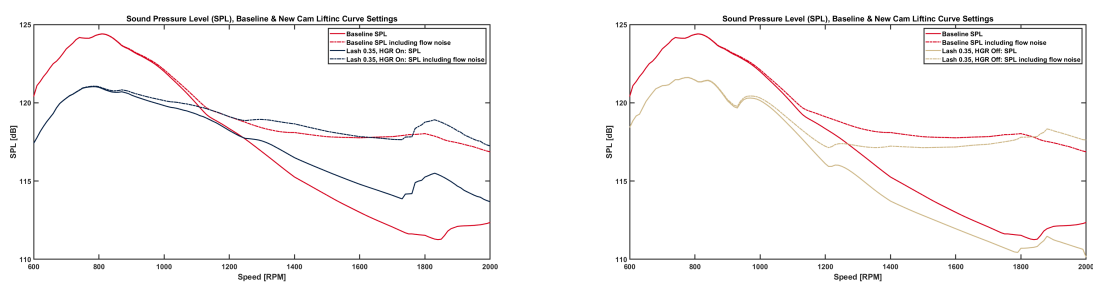


Figure 5.3.1: Baseline and new cam lifting curves for the inlet and exhaust valves (left) and the absolute difference (right)



(a) Sound pressure level, Baseline and New lift curve with HGR On (b) Sound pressure level, Baseline and New lift curve with HGR Off

Figure 5.3.2: Acoustic output, SPL with and without flow noise included for the full speed simulation (600-2000 RPM with step size 10) comparing the results using baseline settings and the new cam lifting curve at optimal lash (0.35 mm on inlet and exhaust) and HGR-valve On (left) and Off (right).

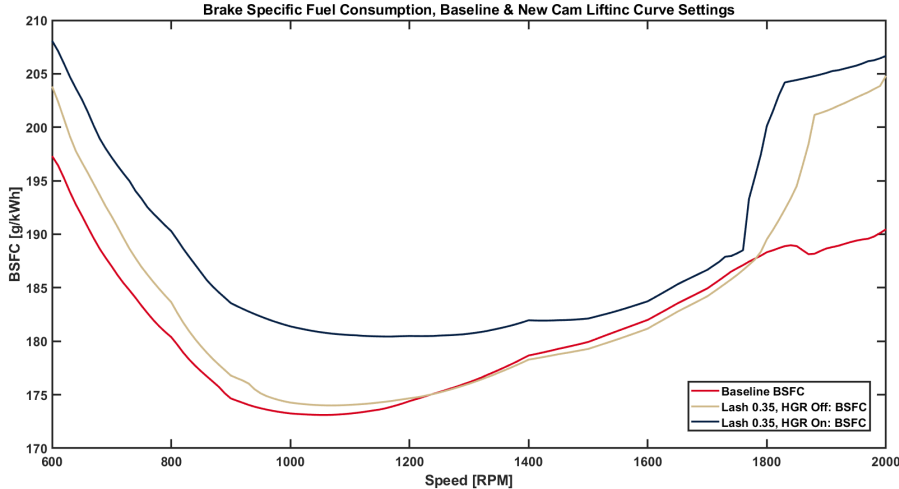


Figure 5.3.3: Brake specific fuel consumption for the full speed simulation (600-2000 RPM with step size 10) comparing the results using the baseline settings and the new cam lifting curve at optimal lash settings (0.35 mm on inlet and exhaust, HGR-valve On and Off).

A profound discussion on the topic and possible effects on the results of this project as well as suggestions for further investigation are found in Section 6.1.2.

5.4 The Optimal Design

According to the results presented within this Section, a suggested optimal design to the optimization problem for this project is presented in Table 5.4.1. Remark that it is only the lash that is considered to have enough impact on acoustics without affecting the overall performance to be changed. The HGR-valve is not suggested to be switched On at any speed due to the increase in fuel consumption (see Section 6.1.2).

The suggested optimal setting considers the new cam lifting curve for the valve lash. The optimal design together with the baseline is thus what is presented in Figure 5.3.2b and for the beige and red curves in Figure 5.3.3. The absolute acoustic reduction over the operating speed range is shown in Figure 5.4.1, showing the difference $C_{old} - C_{new}$.

For the main target of this project, i.e. the acoustic output from the engine itself (SPL without flow noise) at the speeds prioritized (1400-1700 RPM), the optimal design is on average 1.2 dB lower than the baseline. Over the complete operating speed range, the average reduction is 1.69 dB.

Parameter	Optimal Setting
Inlet lash	0.35 mm (New cam lifting curve)
Exhaust lash	0.35 mm (New cam lifting curve)
HGR-valve	Off
Exhaust brake valve	110 mm
Inlet cam timing angle	0 °
Exhaust cam timing angle	0 °
Fuel injection gain	0 %

Table 5.4.1: Suggested optimal settings for each parameter considered.

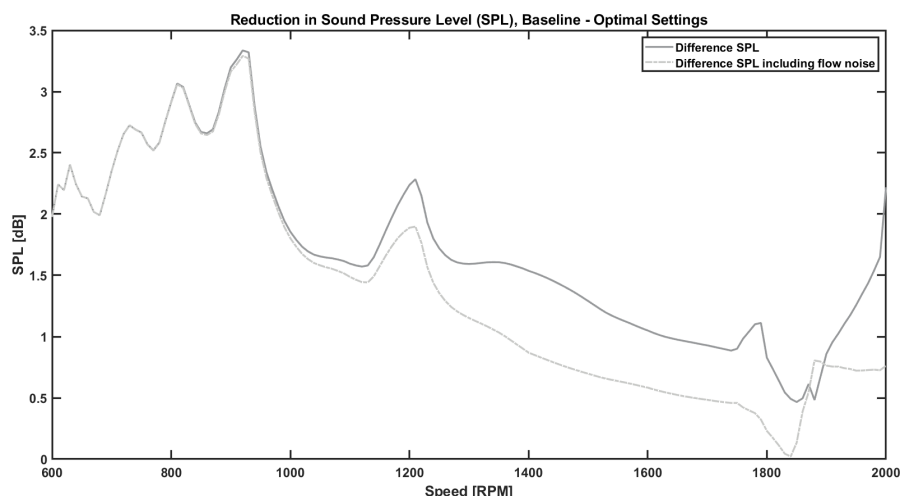


Figure 5.4.1: Difference in sound pressure level for the baseline and the optimal design suggested.

Chapter 6

Discussion and Conclusions

In this section, the results from Section 5 and the working procedure described in Section 4 are discussed and analysed further. From this, final conclusions and suggestions for future work on the topic are presented. The section ends with some final words summarizing the work and the project as a whole.

6.1 Discussion and Conclusions

Given the problem to minimize the acoustic output from the Scania CBE1 engine without impairing overall performance, a first general conclusion can be stated that the noise levels can indeed be improved by adjusting parameter settings.

Another main conclusion is that the simulation model needs re-modification in order to be used properly for the purpose of this study.

6.1.1 Simulation Methods

An important remark is that the results from the first simulation performed using the Design Optimizer has continued to apply throughout the complete project. This may of course simply be because of the choice of parameters investigated in that particular setup, but a valuable conclusion is that a smaller optimization problem can provide valuable results applicable also for the main problem. Throughout this study, the Design Optimizer has overall performed satisfactory and is suggested to be used when considering complex optimization problems. From the mathematical point of view, the

simplicity of using the Design Optimizer to solve such a complex optimization problem is remarkable.

Since one of the main purposes of this study was to develop methods to solve the complex optimization problems, the Design Optimizer was put to test as the complete optimization problem was given all at once. Inaccurate optimization results are not always obvious until the Design Optimizer finishes, thus DoEs are considered a faster and more efficient way to investigate whether or not a possible parameter may be adjusted as desired, before using the Design Optimizer. The accuracy of the results from the Design Optimizer has proven to be better for the smaller optimization problems within this study (regardless the approach used). This also points to use the Design Optimizer on more, but smaller sub-problems rather than simulating one very large one.

The Design Optimizer

The Design Optimizer is considered a useful tool in order to investigate how parameter settings affects the acoustic output. Especially when handling complex optimization problems such as the minimization of noise levels. From the use within this study, the Design Optimizer has provided valuable information about how the optimal designs can be approached. The Design Optimizer is particularly suggested in initial stages of a process to provide valuable information about how the parameters may affect the objective function. Too large problems (here related to the number of design variables) are not suitable without further investigations of adjusted settings of the optimization tool.

The Design Optimizer requires constant network connection and in cases where the connection has been lost, some designs have not been completed properly. This has in some cases caused skipped designs which in turn has led to erroneous numbers on the designs simulated. As the number of skipped designs has been low, the correct number of a specific design has been obvious. Yet, as the optimal design is used for a final simulation yielding more specified results of the complete case, this simulation has been made with a non-optimal design. This error has not caused any problems during this project, but is mentioned as a weakness of the system as it may cause problems in other projects where the final simulation is of greater importance.

For the different optimization approaches investigated (Multi-objective Pareto, Multi-

objective weighted sum, and Single-objective), it is concluded that the Design Optimizer performs well for all three approached used. Regarding the weighted sum approach, a sum of the two objectives (SPL and BSFC) is computed according to equation 2.27. This yields a number that is irrelevant for the continuation of the project and is thus omitted here. Nevertheless, the result of the optimization is satisfactory as the design variables has converged explicitly to reasonable and accurate values within the evolution performed by the Design Optimizer. This could in fact indicate that the acoustic output and the fuel consumption has correlated behaviour for changes of the particular parameters (here, lash and HGR-valve).

Time Complexity

The run time of the larger optimizations within this project (751 designs, four speeds) is approximately three days. The time for setup and remodeling of the simulation model is considered small in this context and does not add much more to the time required. Three days can of course be considered a long time, but compared to physical tests, which is the other option available, both time (considering planning, test setup, verification, etc.) and especially cost is much lower for simulations. Consider also that actual parts may not be available during the development phase which can affect the quality (or increase cost even more) of physical tests. Since the methods used and developed within this study shows satisfactory results, it is considered an efficient way to investigate possible improvements in exhaust system acoustics. Remark also that the efficiency is expected to increase with better routines and users' knowledge which in turn will lead to fewer simulations to be performed.

Non-linearity

The dependency between the different parameters investigated within this study has not been obvious, nor has the investigation of it been prioritized. Still, the Design Optimizer should take the non-linearity into account and comparing with the DoEs, most results appears to be equal when investigating them one by one. Consider though the change in results as the new cam lifting curve is introduced is worth mentioning. Here, the speed at which the HGR-valve affects the acoustic output the most are different for the two lifting curves which shows how new parameter settings changes the optimum for other parameters over the different speeds.

Objective Function

For all except one optimization round, the objective function is set to the SPL including flow noise. If the SPL without flow noise would be set as target instead, a different result might have been derived. With the flow noise excluded, the combustion sound is dominating. As valves controls the gaseous flow and its velocity, many of the parameters within this study could have more impact on the flow noise than the combustion sound. Nevertheless, the flow noise is mainly dependent on the geometry and the velocity of the gases. Here, the geometry of the system is not taken into account (as GT-Power simulations are 1D-simulations), thus the flow noise is only dependent on the gases' velocity. The velocity is in turn a function of mass flow and temperature of the exhaust gases and due to the optimization over the design variables here, these parameters are expected to change due to changes in injected fuel, air intake, temperatures in the engine, etc. The relative effect of noise reduction is also expected to be higher if the noise from the engine itself is reduced rather than the exhaust system where the flow noise dominates. In order to quantify the effects of different parameter settings and since it is not expected to impair the overall result, the objective function is primarily set to be SPL including flow noise.

Constraints

The constraint of the turbo speed is violated at the baseline simulation (Section 5.1). Since the violation is expected to be caused by the altitude difference in the simulation and for the given constraint's conditions, it is considered small enough to be ignored. Nevertheless, if values above the given limit are allowed despite the infringement and the baseline settings are this close to given limits, the constraints should probably have been more generous when using the Design Optimizer. The Design Optimizer classifies a design as infeasible as soon as a constraint is violated and does indeed not allow for any flexibility for infringement. There is by all means a risk that the optimal solution suggested is affected by constraints that might be too tight, and that the result would be different if the feasible region was extended. This is particularly seen in the results of the last optimization performed (Section 5.2.2). Here, the Design Optimizer has failed to find any feasible solutions with the HGR-valve turned Off. Looking into more detail of the suggested designs where the valve is turned off, it is shown that it is most often the turbo speed limit that is violated but that the trampling is very small. Since all other simulations has shown lower acoustic output for HGR-valve turned off, the

outcome of this optimization would most probably be different if the constraint was set wider.

The total effect on this project of the constraints being set with too small margins may nevertheless be considered negligible since results from several simulations has been compared. Still, this must be taken into account when using the Design Optimizer in future work.

6.1.2 Parameter Settings

Out of the parameters investigated and the simulation model used within this study, the valve lash, the HGR-valve, the exhaust brake valve and the fuel injection are possible candidates to be adjusted in order to investigate the acoustic output. Out of these, the valve lash and the HGR-valve are the parameters considered to be adjustable whilst keeping the engine operating properly.

Valve Lash

From all optimization rounds performed (where the results has been considered accurate) the acoustic levels has decreased with smaller valve lash on both inlet and exhaust side of the cylinder. This is regardless of other parameter settings and the result is also confirmed by DoE simulations. It has nevertheless been concluded the actual valve lash using the settings in the baseline model is uncertain (as presented in Section 5). The difference in acoustic output for different valve lash is still considered an important result of the project.

Since the valve lash is suggested to have impact on the noise levels and as it is also considered a component that is relatively simple to adjust on the actual engine, the simulation results using the new cam lifting curve yields interesting conclusions and suggestions for future work. Using the baseline cam lifting curve, the clear conclusion is that the valve lash should be as small as possible in order to reduce noise, but the minimum level can not be determined. For the new cam lifting curve, the same behaviour is expected, but not verified as the new curve was provided late in the process. Consider also that it is not investigated how well the different cam lifting curves represents the actual acoustic output, which thus need to be investigated.

HGR-Valve

The noise level is lower with the HGR-valve On (open) below approximately 1100 RPM. At these lower speeds, there is basically no flow noise present (as seen in Figure 5.1.1) hence the acoustic drop in having the HGR-valve open is not due to how much flow there is in the system. Instead, this is suggested to be caused by a back pressure (negative pressure) on the intake side of the system at lower speeds. (The negative pressure is confirmed by studying the simulated pressure in the system in GT-Post.) Allowing more air to be provided the intake valves by the system itself, e.g. by opening the HGR-valve, the pressure evens out which in turn lowers the acoustics.

Despite the fact that the HGR-valve decreases the noise levels if turned On at speeds below approximately 1100 RPM, the optimal design (presented in Section 5.4) suggests the HGR-valve to be turned Off during the complete operating speed range. Since the range of speed prioritized in this project is not favoured by switching the HGR-valve On, the increase in fuel consumption is considered to predominate the acoustic advantages at the lower speeds.

Exhaust Brake Valve

The first optimization results indicates that closing the exhaust brake valve decreases the acoustic output. This is assumed to be caused by the reduced flow in the system, but is not investigated in detail. Nevertheless, the simulations are setup to imitate the pass-by noise tests conditions, which are performed at 100 % load (i.e. heavily loaded truck travelling uphill). Running the engine under the test conditions with the exhaust brake valve not completely open is not a viable option, why the exhaust brake valve can be excluded from most simulations. The BSFC is not simulated properly for the complete range regarding the exhaust brake valve, but as the acoustic effect is shown and as the engine does not actually operate under the conditions simulated, further investigations are not considered necessary for the purpose of this specific project.

6.2 Future Work

This project was a first attempt to reduce engine noise by adjusting parameter settings using GT-Power simulations. The results indicates weaknesses in the simulation model to complete the acoustic simulations properly. A strong recommendation

for future work would therefore be to re-modify the simulation model in order to enable adjustments that can be of interest for the research area of engine acoustics. The simulation model has been developed with respect to a number of performance requirements. The acoustic output is in general downgraded in favor for fuel efficiency, emission control, cost, performance, etc. When investigating the acoustic output, extreme values (that may not always be practically viable) are sometimes of interest to simulate in order to understand the noise's origin. Re-building of the simulation model may thus be considerable in order to better examine parameters such as the cam timing angle. Changing the cam timing angle has shown promising results in physical test, why re-modifications in order to solve for different cam timing angles is suggested to be prioritized.

The significant difference in acoustic output as the new cam lifting curve is provided yields questions of how other parameters and settings may be managed in similar ways to improve accuracy. This is of course interesting topics for future work and could possibly be considered together with the re-modification suggested above. As the quality of the simulation improves, more components could be investigated as well. Further on, and as more accurate simulation results are generated, physical test are suggested in order to verify the simulation results. In order to better understand the acoustic output of the exhaust system, the simulated noise can be analyzed further by selecting different simulation results in GT-Power. For example, the engine orders could be considered to be investigated further to better understand in which frequency ranges the noise reduction appears.

As already mentioned, reconsideration of the components investigated and re-modelling of the simulation model has been required throughout this project. Therefore, more advanced settings of the Design Optimizer has not been possible to investigate further within this study. This is thus suggested for future work in order to find better settings to improve the results from the Design Optimizer. For example, a comparison of the results using different target functions (one out of equations 2.24) could possibly yield different results. By analyzing the data provided from the optimizations, much can be concluded about how the acoustic output has evolved during the different designs simulated. Yet, the possible effect on the optimization results can still not be evaluated properly. For future work, an optimization targeting to minimize the largest function instead of the smallest would be recommended initially, since that is expected to yield the biggest difference (if any) from the result provided

here. Also, to minimize the maximum value instead is suggested to give a more robust solution and possibly reduce complexity of the optimization problem. Nevertheless, for the speed range covered within the optimization simulations here (1400-1700 RPM), the acoustic output differs over the four speeds in a somewhat linear way. Thus, the target function will possibly not change the overall results for this project, but could still play a more important role in other setups.

6.2.1 Component Settings

HGR-valve

The reason to the noise decrease caused by the opening of the HGR-valve at lower speeds is, as already mentioned, possibly due to the back pressure in the system. This back pressure is favorable in terms of performance, but not when considering acoustics. Nevertheless, the significant drop in SPL about 800 RPM is certainly something that can be investigated further, especially as the highest overall noise levels are measured here. It is also within this area booming noise¹ appears. Booming noise is deteriorating the driver's experience and comfort why eliminating it is of great importance when developing premium brand trucks. It may therefore be interesting to further investigate how the back pressure and the noise are correlated and if the extra gaseous flow could be provided in another way that does not affect the fuel consumption to such a high extent.

The effects of switching the HGR-valve On or Off investigated are considered enough to determine whether the HGR-valve should be On or not from an acoustic and fuel consumption perspective. The effect on emission of nitrogen oxides (NO_x) is not at all considered within this project and is thus a recommendation for further research.

Fuel Injection

Figure 5.2.13 shows results for four speeds, 600, 1100, 1500 and 2000 RPM. Note here the different behaviour in acoustic output at 1100 RPM (5.2.13b) compared to the other speeds simulated. All parameters examined here has not been investigated to the desired level due to prioritization. It is therefore suggested to further investigate the effect of fuel injection adjustments. The effect seems to vary over different speeds

¹An increase of sound intensity due to pure or narrow band tones related to the firing frequency of the engine and how the harmonics excite the passenger cavity. [24]

which in deed should be investigated further. For the speed range prioritized here, the acoustic output shows only small fluctuations as the amount of fuel injected is varied. Also, as the operating rhythm can be impaired by uneven fuel injection, the parameter's effect was downgraded here as other parameters were considered more important.

6.3 Final Words

This thesis project has been the first attempt to investigate acoustic problems from an engine design perspective. Thus, it has changed direction during the process as new possibilities or limitations has been discovered. Engine acoustic is a wide research field, including many sub-areas such as pure acoustic, engine development, systems engineering and, in order to solve minimization problems as attempted here, mathematical optimization. This thesis project is mainly focused on systems engineering and optimization, thus the main research has focused on that. Nevertheless, in order to qualitatively analyze the results from the simulations performed, acquisition of knowledge outside the main research area has been required. The results are considered important for Scania and from a general engine acoustic perspective in order to further develop the research in engine acoustics. From an optimization and systems engineering perspective, valuable conclusions has been drawn for the use of optimization tools to solve optimization problems within a very complex system, such as the IC engine.

Appendix - Contents

A Additional results	71
A.0.1 Single Optimization	71
A.0.2 Multi-Objective Weighted Sum	72
A.0.3 Valve Lash DoEs	72

Appendix A

Additional results

Here, further result plots from additional optimizations and simulations are presented.

A.0.1 Single Optimization

Results from single optimization over inlet and exhaust valve lash as well as the HGR-valve for 600, 1100 and 2000 RPM are seen in Figure A.0.1. Specifications of the suggested optimal settings are presented in Table A.0.1.

Speed	Parameter	Suggested Optimal Setting
600 RPM	Inlet valve lash	0 mm
	Exhaust valve lash	0 mm
	HGR-valve	On
1100 RPM	Inlet valve lash	0 mm
	Exhaust valve lash	0 mm
	HGR-valve	Off
2000 RPM	Inlet valve lash	0 mm
	Exhaust valve lash	0 mm
	HGR-valve	Off

Table A.0.1: Suggested optimal settings with the weighted sum approach at 1500 RPM.

APPENDIX A. ADDITIONAL RESULTS

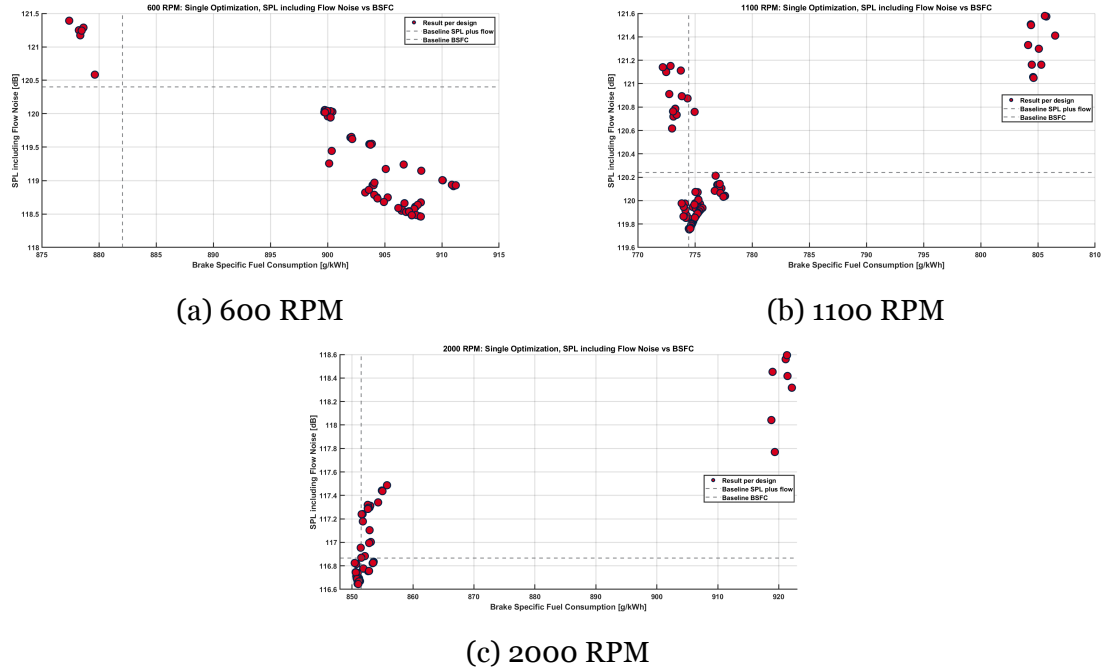


Figure A.o.1: Optimization results for single optimization regarding valve lash and HGR-valve.

A.0.2 Multi-Objective Weighted Sum

A Pareto front of the multi-objective optimization using the weighted sum approach is presented in Figure A.o.2.

A.0.3 Valve Lash DoEs

Simulation results for the acoustic output from DoEs where the inlet and exhaust valve lash are varied between 0 mm and 0.5 mm at additional speeds. Design 1 corresponds to 0 mm lash on both inlet and exhaust valves. Following designs corresponds to larger valve lash until Design 25 where both inlet and exhaust valve lash is 0.5 mm. The results for 600 RPM, 1100 RPM and 2000 RPM are seen in Figure A.o.3

APPENDIX A. ADDITIONAL RESULTS

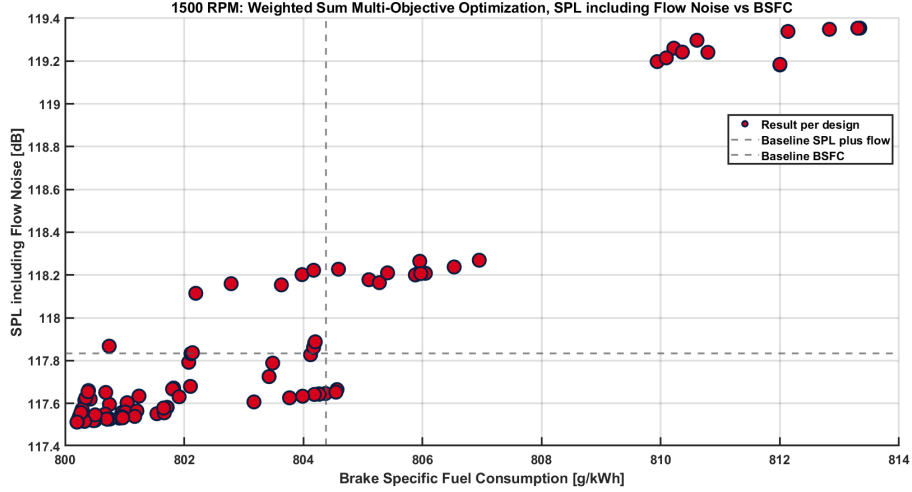


Figure A.o.2: Multi-objective optimization results with the weighted-sum approach.

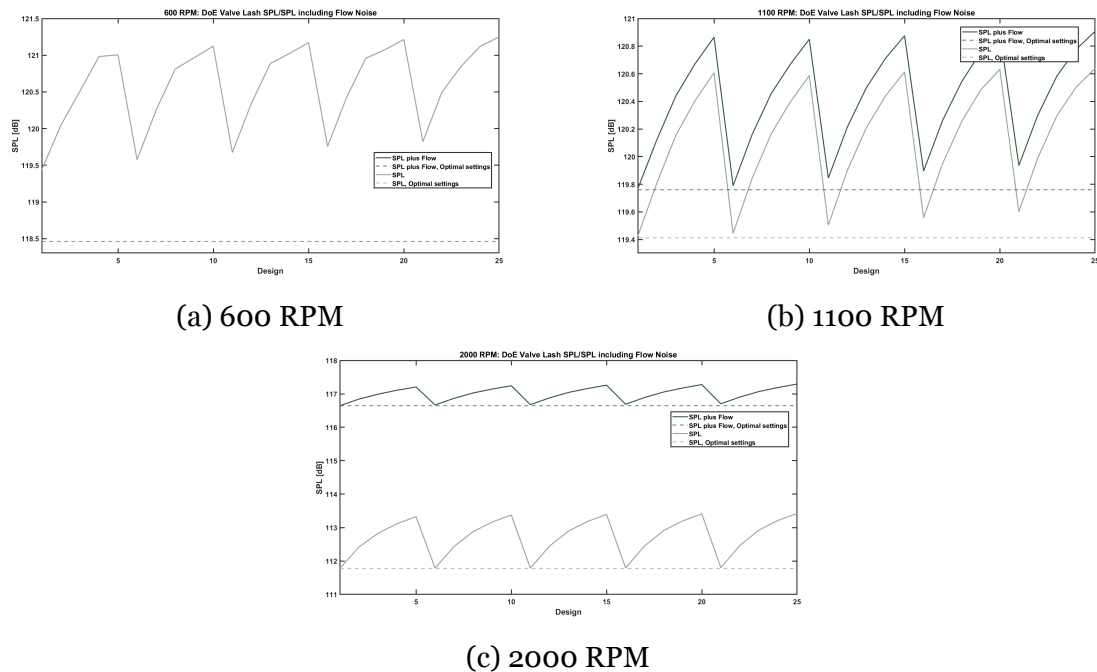


Figure A.o.3: Acoustic output (SPL including and excluding flow noise) from DoE simulations where inlet and exhaust valve lash are varied over different speeds.

Bibliography

- [1] Blondel, Vincent D. and Tsitsiklis, John N. "A Survey of Computational Complexity Results in System Control". In: Automatica, Volume 36, Issue September 2000, Pages 1249-1274 (1999). DOI: 10.1016/S0005-1098(00)00050-9. URL: [https://doi.org/10.1016/S0005-1098\(00\)00050-9](https://doi.org/10.1016/S0005-1098(00)00050-9).
- [2] Blundell, Stephen J. and Blundell, Katherine M. Concepts in Thermal Physics, Second edition. Oxford University Press, 2017. Chap. 14, p. 140. ISBN: 978-0-19-956209-1.
- [3] Broatch, A., Novella, R., Gomez-Soriano, J., Pinaki, P., and Som, S. "Numerical Methodology for Optimization of Compression-Ignited Engines Considering Combustion Noise Control". In: SAE International Journal of Engines, Volume 11, Issue 6, Pages 625-642 (2018). ISSN: 1946-3936. DOI: 10.4271/201-01-0193.
- [4] Charles, Vann Loan. Computational Frameworks for the Fast Fourier Transform. SIAM - Society for Industrial and Applied Mathematics, 1992. Chap. 1, pp. 1–11. ISBN: 978-0-898712-85-8. URL: <https://pubs-siam-org.focus.lib.kth.se/doi/pdf/10.1137/1.9781611970999.fm>.
- [5] Collette, Yann and Siarry, Patrick. Multiobjective Optimization. Principles and Case Studies. Springer-Verlag Berlin Heidelberg, 2004. Chap. Forewords, p. 7. ISBN: 978-3-662-08883-8.
- [6] Deb, K. and Jain, H. "An Evolutionary Many-Objective Optimization Algorithm Using Reference-point Based Non-dominated Sorting Approach, Part I: Solving Problems with Box Constraints". In:

- IEEE Transactions on Evolutionary Computation, Volume 18, Issue 4, Pages 577-601 (2014). DOI: 10.1109/TEVC.2013.2281535. URL: <https://ieeexplore.ieee.org/document/6600851?arnumber=6600851>.
- [7] Donavan,
Paul R. and Schumacher, Richard. Handbook of Noise and Vibration Control. Ed. by Malcolm J. Crocker. 2007. Chap. 120, Exterior Noise of Vehicles—Traffic Noise Prediction and Control, pp. 1427–1437. ISBN: 9780470209707. DOI: 10.1002/9780470209707. URL: <https://doi-org.focus.lib.kth.se/10.1002/9780470209707.ch120>.
- [8] Environmental Noise Guidelines for the European Region.
World Health Organisation Regional Office for Europe, 2018. Chap. 1, pp. 1–3. ISBN: 978-92-890-5356-3. URL: https://www.euro.who.int/__data/assets/pdf_file/0008/383921/noise-guidelines-eng.pdf.
- [9] Francis, Clinton D., Ortega, Catherine P., and Cruz, Alexander. “Noise Pollution Changes Avian Communities and Species Interactions”. In: Current Biology, Volume 19, Issue 16, Pages 1415-1419 (2009). DOI: /10.1016/j.cub.2009.06.052. URL: <https://doi.org/10.1016/j.cub.2009.06.052>.
- [10] Ginsberg, Jerry H.
Acoustics - A Textbook for Engineers and Physicists. Volume I: Fundamentals. Springer International Publishing AG, 2021. Chap. 1. ISBN: 978-3-319-56844-7. DOI: 10.1007/978-3-319-56844-7.
- [11] Glad, Torkel
and Ljung, Lennart. Reglerteknik. Grundläggande teori. Studentlitteratur AB, 2006. Chap. 1.6, pp. 20–21. ISBN: 978-91-44-02275-8.
- [12] GT Suite. 2021. URL: <https://www.gtisoft.com/> (visited on 11/16/2021).
- [13] GT-Suite Acoustics Application Manual. Gamma Technologies LLC, 2021.
- [14] GT-Suite Engine Performance Application Manual. Gamma Technologies LLC, 2021.
- [15] GT-Suite Optimization Manual. Gamma Technologies LLC, 2021.
- [16] Hansen, Colin H. Fundamentals of Acoustics. 2016. URL: https://www.who.int/occupational_health/publications/noise1.pdf?ua=1 (visited on 11/11/2021).

BIBLIOGRAPHY

- [17] Hansen, Nikolaus. “The CMA Evolution Strategy: A Tutorial”. In: (2016). arXiv: 1604.00772 [cs.LG]. URL: <https://arxiv.org/abs/1604.00772>.
- [18] Heywood,
John B. Internal Combustion Engine Fundamentals, Second Edition. McGraw-Hill Education, 2018. ISBN: 978-1-26-011610-6. URL: <https://www-accessengineeringlibrary.com.focus.lib.kth.se/content/book/9781260116106>.
- [19] Münzel, Thomas, Schmidt, Frank P., Steven, Sebastian, Herzog, Johannes, Daiber, Andreas, and Sørensen, Mette. “Environmental Noise and the Cardiovascular System”. In: Journal of the American College of Cardiology, Volume 71, Issue 6, Pages 688-697 (2018). DOI: 10.1016/j.jacc.2017.12.015. URL: <https://doi.org/10.1016/j.jacc.2017.12.015>.
- [20] Nocedal, Jorge and Wright, Stephen J. Numerical Optimization. 2nd ed. Springer Science+Business Media, 2006. Chap. 9.5, pp. 238–240. ISBN: 978-0387-30303-1.
- [21] “REGULATION (EU) No 540/2014 OF THE EUROPEAN PARLIAMENT AND OF THE COUNCIL of 16 April 2014. on the sound level of motor vehicles and of replacement silencing systems, and amending Directive 2007/46/EC and repealing Directive 70/157/EEC, 2019”. In: (). URL: <https://eur-lex.europa.eu/legal-content/EN/TXT/?uri=CELEX%5C%3A02014R0540-20190527>.
- [22] Rossing, Thomas D. and Fletcher, Neville H. Principles of Vibrations ans Sound, Second Edition. Springer-Verlag Berlin Heidelberg, 2004. ISBN: 978-1-4419-2343-1.
- [23] Scania Super. 2021. URL: <https://www.scania.com/se/sv/home/campaigns/super.html> (visited on 11/11/2021).
- [24] Shin, Sung-Hwan, Ih, Jeong-Guon, Hashimoto, Takeo, and Hatano, Shigeko. “Sound Quality Evaluation of the Booming Sensation for Passenger Cars”. In: Applied Acoustics, Volume 70, Issue 2, February 2009, Pages 309-320 (2008). URL: <https://doi.org/10.1016/j.apacoust.2008.03.009>.
- [25] Sparr, Gunnar and Sparr, Annika. Kontinuerliga System. 2:8. Studentlitteratur, 2012. Chap. 1, pp. 22–23, 41. ISBN: 978-91-44-01355-8.

BIBLIOGRAPHY

- [26] Yang, Kee-Young, moon, Hyeonchae, han, SangWeol, and Cho, Jae Seol. “A Performance Design of Constant Pressure Type Exhaust Brake”. In: SAE Technical Paper 2021-01-0398 (2021). DOI: 10 . 4271 / 2021 - 01 - 0398. URL: <https://doi.org/10.4271/2021-01-0398>.

TRITA-SCI-GRU 2021:390